This article has been accepted for publication in a future issue of this journal, but has not been fully edited. Content may change prior to final publication. Citation information: DOI 10.1109/TDSC.2022.3141391, IEEE Transactions on Dependable and Secure Computing



# Securely Outsourcing Neural Network Inference to the Cloud with Lightweight Techniques

Xiaoning Liu, Yifeng Zheng, Xingliang Yuan, and Xun Yi

**Abstract**—Neural network (NN) inference services enrich many applications, like image classification, object recognition, facial verification, and more. These NN inference services are increasingly becoming an essential offering from cloud computing providers, where end-users' data are offloaded to the cloud for inference under a customized model. However, current cloud-based inference services operate on clear inputs and NN models, raising paramount privacy concerns. Individual user data may contain private information that should always remain confidential. Meanwhile, the NN model is deemed proprietary to the model owner as model training requires substantial resources. In this paper, we present, tailor, and evaluate `Sonic`, a lightweight secure NN inference service delegated in the cloud. `Sonic` leverages the cloud computing paradigm to fully outsource the secure inference, freeing end devices and model owners from being actively online for assistance. `Sonic` guards both user input and model privacy along the whole service flow. We design a series of secure and efficient NN layer functions purely using lightweight cryptographic primitives. Extensive evaluations demonstrate that `Sonic` achieves up to $60\times$ bandwidth saving in online inference compared to prior art.

**Index Terms**—Secure outsourcing, cloud computing, privacy preservation, neural network inference

## 1 Introduction

Neural network inference services provide ready-made intelligence for end-user applications and help enterprises improve their business, ranging from image classification to face detection [1]. With the wide adoption of cloud computing in various domains (e.g., [2], [3], [4]), these inference services have rapidly become an appealing offering from cloud service providers to empower many applications. Consider a typical application of face detection, where an end-user wishes to evaluate a personal photo under an enterprise's neural network. Due to the well-understood benefits, the enterprise takes advantage of cloud computing service (like Google Vision [5]), where both the end-user photo and model are offloaded to the cloud. The inference service takes place on the cloud which then returns the result to the end-user.

Such practices seem appealing, yet raises critical privacy concerns, posing hurdles to the practical deployment of the service. The raw user data processed by these services often carry private information, such as biometrics and locations [6]. To ensure individuals' privacy, such data should be kept confidential at any time and not be disclosed to cloud in cleartext. Meanwhile, NN models are deemed as intellectual properties and embed traces of (sensitive) training data [7], [8]. Privacy protection of the private user data and proprietary models is thus of paramount importance and necessary in pushing forward the practical deployment of inference services in the cloud [9], [10].

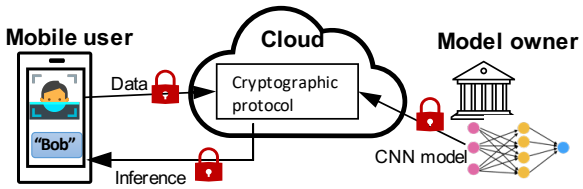


Fig. 1. A secure CNN-powered inference in the cloud. The lock indicates that the data is deployed in encrypted form.

Towards this pressing need, there have been growing research endeavors on leveraging generic cryptographic techniques (such as garbled circuits and homomorphic encryption) to build secure NN inference systems [11], [12], [13]. These systems proceed by encrypting user input data and/or an owner's model, and execute NN inference over encrypted data. Unfortunately, they are still unsatisfactory for practical deployment. Specifically, during the online secure inference, they all need to involve the aforementioned heavyweight cryptographic techniques, and some of them require active user aids throughout the whole inference procedure. Namely, end-users need to continually engage in online interactions and have *symmetric* computing capabilities to the server, in the case that the server holds the plaintext model. These limitations are further aggravated in resource-constrained mobile or embedded user devices.

In light of above observations, in this paper, we propose, implement, and evaluate `Sonic`, a lightweight secure NN inference system running in the cloud. `Sonic` is designed to support Convolutional Neural Networks (CNN), one of the most popular and powerful deep learning models. As shown in Fig. 1, `Sonic` offloads the entire secure inference computation to the cloud. Using such a system framework, `Sonic` mediates the resource limitation of the mobile user and the privacy-invasive cloud: it frees the resource-


- *Xiaoning Liu and Xun Yi are with the School of Computing Technologies, RMIT University, Melbourne, VIC 3001, Australia. Email: xiaoning.trust@gmail.com, xun.yi@rmit.edu.au.*
- *Yifeng Zheng is with the School of Computer Science and Technology, Harbin Institute of Technology, Shenzhen, China. Email: yifeng.zheng@hit.edu.cn.*
- *Xingliang Yuan is with the Faculty of Information Technology, Monash University, Clayton, VIC 3800, Australia. Email: Xingliang.Yuan@monash.edu.*
- *Corresponding author: Yifeng Zheng.*

This article has been accepted for publication in a future issue of this journal, but has not been fully edited. Content may change prior to final publication. Citation information: DOI 10.1109/TDSC.2022.3141391, IEEE Transactions on Dependable and Secure Computing



constrained mobile user from always staying online; and allows the model owner to dynamically fine-tune their service with an updated NN model without reinstalling the application. At the same time, both the private user data and proprietary CNN model are well protected against the untrusted cloud. In particular, we design a delicate secure inference protocol purely from lightweight secret sharing techniques to foster a low-latency service with judicious usage of network resources. Our contributions can be summarized as follows.

- We design a secure cloud-based outsourced service `Sonic` that supports lightweight secure CNN inference, with protection of both the private user data and the proprietary CNN model. By combining the advancements from system, cryptography, and machine learning literature, `Sonic` enables a full-fledged cloud service framework that can support generic CNN models and provide high-performance inference service.
- We devise a series of efficient secure layer functions fully resorting to lightweight secret sharing. They are essential building blocks for CNN inference, including the secure convolutional layer (SCONV), secure batch normalization (SBN), secure ReLU activation (SReLU), and secure max pooling layer (SMP). We decompose these secure layer functions into smaller and composable cryptographic gadgets, and carefully devise each gadget to optimize the performance of secure NN inference on the cloud.
- We integrate the developed secure functionalities and apply them to four realistic CNN models over benchmarking datasets for extensive evaluation. Results validate the efficiency of `Sonic`, showing that `Sonic` produces a prediction in 0.7s on MNIST with 97% accuracy and in 1.5min on CIFAR-10 with 80% accuracy. Compared with prior art, `Sonic` can achieve up to 60× bandwidth saving in the online inference procedure.

The rest of this paper is organized as follows. Section 2 introduces some preliminaries. Section 3 presents the system architecture and threat model. Section 4 introduces the proposed secure inference protocol. Section 5 analyzes the security. Section 6 presents the experiments. Section 7 investigates the related work. Section 8 concludes this paper.

## 2 Preliminary: Additive Secret Sharing

We now introduce the core cryptographic primitive used `Sonic`— additive secret sharing. Additive secret sharing [14] protects an $\ell$-bit secret value $x$ by additively splitting it in the ring $\mathbb{Z}_{2^\ell}$ as $\langle x\rangle_0^A$ and $\langle x\rangle_1^A$ such that $\langle x\rangle_0^A + \langle x\rangle_1^A \equiv x \pmod{2^\ell}$. Each individual secret share is a uniformly distributed random value in $\mathbb{Z}_{2^\ell}$ and can perfectly hide the information about $x$. Given the shares of two secret values $x$ and $y$, some computation among two parties (denoted as $P_0$ and $P_1$), each of which obtains a share of the values, can be supported as follows. Firstly, addition/subtraction over shares ($\langle z\rangle_i^A = \langle x\rangle_i^A \pm \langle y\rangle_i^A$) and multiplication by a public value ($\langle z\rangle_i^A = \eta \cdot \langle x\rangle_i^A$) can be efficiently evaluated by each party $P_i$ ($i \in \{0,1\}$) at local with no interaction.

Multiplication over two shares ($\langle z\rangle^A = \langle x\rangle^A \cdot \langle y\rangle^A$) requires the assistance of a pre-computed secret-shared multiplication triple $(a,b,c)$ [15], where $c = a \cdot b$. Such triples are data independent and can be generated offline by a third party [16], [17]. As such, `Sonic` assumes the secret-shared triples are already available during the online service. With the secret-shared triple, secure multiplication can be supported as follows. Each party $P_i$ first sets $\langle e\rangle_i^A = \langle x\rangle_i^A - \langle a\rangle_i^A$ and $\langle f\rangle_i^A = \langle y\rangle_i^A - \langle b\rangle_i^A$. Then both parties interact to reconstruct $e$ and $f$. Party $P_i$ then sets $\langle z\rangle_i^A = i \cdot e \cdot f + f \cdot \langle a\rangle_i^A + e \cdot \langle b\rangle_i^A + \langle c\rangle_i^A$.

It is noted that for the special case $l = 1$, additive secret sharing is over $\mathbb{Z}_2$. In this case, the above addition and multiplication operations are replaced with boolean operations XOR ($\oplus$) and AND ($\wedge$) respectively. We denote the boolean sharing of a secret value $x$ in $\mathbb{Z}_2$ as ($[\![x]\!]_0$, $[\![x]\!]_1$). We summarize the key notations in Table 1.

TABLE 1
Key Notations

| Notation | Description |
|---|---|
| $\mathbf{X}, X, \mathbf{x}$ | Input/activation tensor, matrix, and vector. |
| $\mathbf{W}, W, \mathbf{w}$ | Weight tensor, matrix, and vector. |
| $\mu, \delta, \gamma, \beta$ | Batch normalization parameters: the running mean, running variance, scale, and shift. |
| $\ell$, $n$ | Bit length $\ell$ and vector length $n$. |
| $x_k, \mathbf{x}_k$ | The $k$-th element of vector $\mathbf{x}$; The $k$-th vector. |
| $\in_R$ | Uniformly random sampling from a distribution |
| $\langle x\rangle_i^A$ | Arithmetic shares of value $x$ held by server $i$ |
| $[\![x]\!]_i$ | Boolean shares of value $x$ held by server $i$ |
| $\langle x\rangle_i^A \pm \langle y\rangle_i^A$ | Addition/subtraction over arithmetic shares |
| $\langle x\rangle^A \cdot \langle y\rangle^A$ | Multiplication over arithmetic shares |
| $[\![x]\!]_i + [\![y]\!]_i$ | Bitwise XOR over Boolean shares |
| $[\![x]\!] \cdot [\![y]\!]$ | Bitwise AND over Boolean shares |

## 3 System Overview

### 3.1 Architecture

Fig. 2 shows `Sonic`'s system architecture. There is a cloud-based service platform operated by two distinct servers $S_0$ and $S_1$ from independent cloud providers (like Amazon Rekognition [18] and Google Vision [5]) to jointly provide efficient secure neural network inference services. Through the service, a *model owner* holding a proprietary CNN model can deploy the model in protected form on the cloud, which can then provide inference services without seeing the model in cleartext. In practice, the model owner can be a mobile application developing company who have spent massive resources in training the model for a certain application like image recognition with its private customers' data. `Sonic` supports a *mobile user*, who runs an ML-powered mobile application collecting user data, to get inference results without disclosing the confidential or sensitive user data. `Sonic`'s cloud-aided architecture frees the resource-constrained mobile user from storing large models on local device or continuously engaging in the secure inference. Meanwhile, it facilitates the model owner to dynamically fine-tune its service, where the neural network model can be regularly updated without republishing the mobile application.

**Execution flow.** At a high level, `Sonic` works as follows: The model owner protects a pre-trained CNN model $\mathbf{W}$ by the secret sharing technique, generating secret shares $\langle \mathbf{W}\rangle_0^A$ and $\langle \mathbf{W}\rangle_1^A$. Then, $\langle \mathbf{W}\rangle_0^A$ and $\langle \mathbf{W}\rangle_1^A$ are deployed on the cloud servers $S_0$ and $S_1$ respectively. Once the mobile

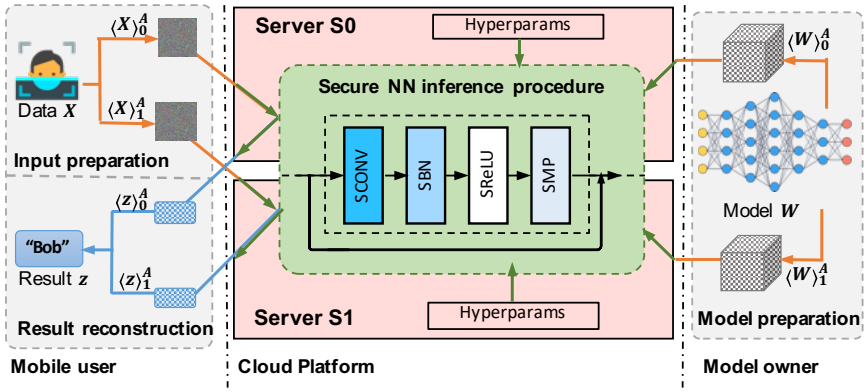


Fig. 2. System architecture.

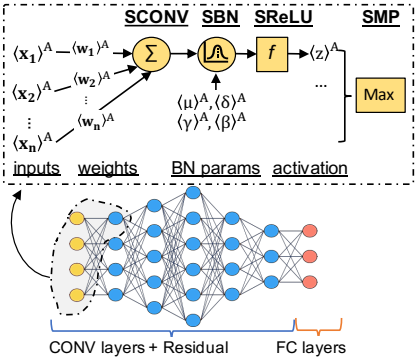


Fig. 3. Sonic's secure layer functions.

user's request arrives at the user interface (on the left of Fig. 2), Sonic protects the raw input (e.g., facial image) as secret-shared tensors $\langle \mathbf{X} \rangle_0^A$ and $\langle \mathbf{X} \rangle_1^A$ and feeds them into the secure service hosted in corresponding cloud servers. The cloud servers run Sonic's secure inference procedure collaboratively (green box in Fig. 2) and send the secret-shared output $\langle \mathbf{z} \rangle_0^A$ and $\langle \mathbf{z} \rangle_1^A$ to the mobile user. The mobile user then combines the shares and produces the inference result $\mathbf{z}$ labeling the class of user input.

### 3.2 Threat Model and Privacy Goals

We consider that the threats in Sonic mainly come from the engagement of the cloud servers that jointly provide the secure inference service. Following prior works in the two-server model [16], [19], [20], we assume that the cloud servers are semi-honest and non-colluding. They will honestly follow our protocol, yet attempt to infer private information beyond their access rights. The rationale behind such assumption is that cloud providers are well-established companies and not willing to harm their reputation, thus avoiding behaving maliciously and collusion [21]. It is noted that such multi-server model has become increasingly appealing in many industrial projects as well. Examples include privacy-preserving ML frameworks like Facebook's CrypTen [22] and Cape Privacy's TFEncrypted [23].

Sonic aims to ensure that both the private data of the mobile user and the (trained) parameters of the model are hidden from the cloud servers. Through interaction with the cloud servers, the mobile user only learns the inference result and nothing else. Consistent with prior works [11], [13], [19], [20], Sonic does not hide the architecture information (hyperparameters) of the model, such as dimension of weight tensor and number of layers. Last, like most prior works on secure inference [11], [12], [13], [19], [20], [24], Sonic does not aim to protect against adversarial machine learning attacks. Such attacks [7], [8], [25], [26] may attempt to exploit the inference procedure as a blackbox oracle to infer information about the training dataset or the model. Mitigating these adversarial ML attacks is orthogonal to Sonic's security scope, as per the definition of secure multi-party computation. Defenses against these attacks are complementary and active research areas, such as differentially private learning [27], [28], [29], [30], modification of NN models [25], [31], [32], and query auditing [33], [34]. We refer the readers to Section 7.3 for more detailed discussion.

## 4 Our Proposed Design

In this section, we present a series of secure layer functions as the main building blocks of secure NN inference in Sonic. Fig. 3 depicts the typical computational blocks in CNN and their secure counterparts, including the secure convolutional layer (SCONV), the secure batch normalization (SBN), the secure ReLU activation (SReLU), and the secure max pooling layer (SMP). These secure layers are organized in pipeline, where each layer receives an encrypted input and produces a desired encrypted output to the next layer. Sonic decomposes each layer into smaller and composable units (i.e., cryptographic gadgets) while preserving its security guarantees. Each unit is customized to be amiable for secret sharing techniques, so as to enable efficient and low-bandwidth execution of secure NN inference. For the most challenging ReLU and Max Pooling layers, we leverage insights from the digital circuit design literature and construct a highly efficient secure comparison gadget purely resort to lightweight boolean sharing techniques. With all these designs, our experiment results (Section 6) show that Sonic can achieve up to $60\times$ bandwidth saving compared with prior art.

### 4.1 Setup

Sonic's secure designs proceed in the ring $\mathbb{Z}_{2^\ell}$. Initially, all mobile user input and model weights need to be converted to integers, so that they can be secretly shared over $\mathbb{Z}_{2^\ell}$. Sonic adopts the fixed-point representation to handle real-valued numbers. As Fig. 4 shows, each real-valued data $x$ is rounded and scaled into an integer $\bar{x} \bmod 2^\ell$, where a two's complement is used to represent the negative values. The most significant bit (MSB) indicates the sign (1→negative; 0→positive). Such signed integer $\bar{x}$ can be shared over $\mathbb{Z}_{2^\ell}$, where the lower-half $[0, 2^{\ell-1}-1]$ represents the non-negative values and the upper-half $[2^{\ell-1}, 2^\ell - 1]$ represents the negative values. Both data value and its sign are well protected. Multiplication over two fixed-point numbers can lead to a $2^{2q}$ scaling factor ($2q$ fractional bits) for the resulting product, which exceeds the bit-length $\ell$ of the ring $\mathbb{Z}_{2^\ell}$.

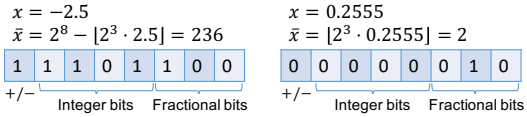


Fig. 4. Examples of the fixed-point representation for signed number, where $\ell = 8, q = 3$.

To ensure the computation correct, all intermediate results should be scaled down by $2^q$ before proceeding the succeeding operation. Sonic adopts a secure local truncation scheme [19] which simply discards the last $q$-bit fractional part to adjust the product to $\ell$ bits. Similar treatment also appears in prior works [13], [35].

Based on this fixed-point representation, the client converts its task-specific raw input to a tensor $\mathbf{X}$ and produces additive shares of every data point. It then dispatches the corresponding shares to cloud servers $S_0$ and $S_1$ which then pad these shares with 0 to fit with the kernel size. The model owner produces additive shares of its CNN model tensor $\mathbf{W}$. To support efficient secure batch normal function, the model owner first derives two set of parameters $\epsilon_1 = \gamma/\delta, \epsilon_2 = \beta - \gamma\mu/\delta$ from the BN parameters: the running mean $\mu$, the running variance $\delta$, the scale $\gamma$, the shift $\beta$. It then produces additives shares of its CNN model tensor $\mathbf{W}$ (kernels and $\epsilon_1, \epsilon_2$). To this end, the model owner deploys the shares of weights to the cloud servers.

### 4.2 Secure Linear Layers

In this section, we present the secure realizations of linear layers, i.e., the secure convolutional layer (SCONV) and the secure fully connected layer (SFC). Their functionality can be expressed as

$$z = f(\mathbf{x}, \mathbf{w}) + bias;$$
$$f(\mathbf{x}, \mathbf{w}) = \mathsf{VDP}(\mathbf{x}, \mathbf{w}) = \Sigma_{k=1}^{n} w_k \cdot x_k, \quad (1)$$

which work over the $n$-dimensional layer input vector $\mathbf{x}$ (or the activation vector for hidden layers) and weight vector $\mathbf{w}$, plus the $bias$ attached on each neuron. In Sonic, we introduce the main building block, i.e., the secure VDP function (SVDP), to realize the above Eq. 1 in the secret sharing domain. Here, we make an important observation from the known literature [36] and open source framework [37] that the bias can be removed if applying batch normalization, because the shift $\beta$ in BN achieves the same effect as the bias. Likewise, we set the bias as 0 to avoid the involvement of real-valued bias and make our design more compatible with the secret sharing techniques.

**Secure VDP.** The secure VDP function (SVDP) computes the convolution operation for conventional CNNs in Eq. 1. It takes as input a set of secret shares of input vector as $\langle \mathbf{x} \rangle_i^A$ and weight vector as $\langle \mathbf{w} \rangle_i^A$, respectively, and outputs the secret shares of their VDP result $\langle z \rangle_i^A$, where $i \in \{0, 1\}$ is the identifier of the two cloud servers $S_0, S_1$. The vector $\mathbf{x}$ can be the activation output from previous ReLU function or represent the raw input of user. The $\mathsf{SecVDP}(\langle \mathbf{x} \rangle_i^A, \langle \mathbf{w} \rangle_i^A)$ proceeds among the two cloud servers $S_0$ and $S_1$ as follows:

1) For $k \in [1, n]$, $S_0$ and $S_1$ jointly compute the element-wise multiplication $\langle z_k \rangle^A = \langle x_k \rangle^A \cdot \langle w_k \rangle^A$.
2) $S_i$ locally sums the products $\langle z \rangle_i^A = \sum_{k=1}^{n} \langle z_k \rangle_i^A$.

### 4.3 Secure Batch Normalization

Batch normalization [36] performs element-wise normalization on each neuron's feature $a$ via

$$\hat{a} = (a - \mu)/\sigma, z = \gamma \cdot \hat{a} + \beta, \quad (2)$$

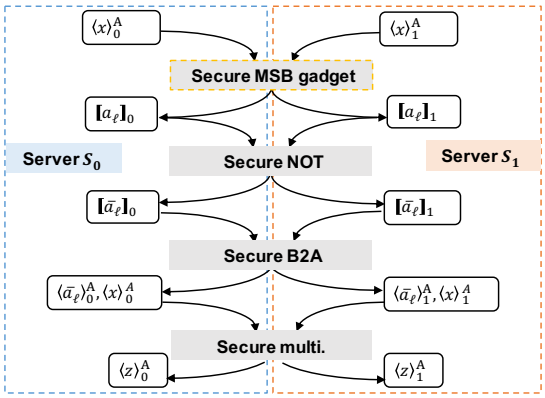


Fig. 5. An overview of the SReLU function.

where $\mu$ is the *running mean* and the non-zero $\sigma$ is *running variance* of the training dataset; and $\gamma$, $\beta$ are the *scale*, the *shift* parameters. The secure batch normalization function (SBN) is applied on each neuron right after the secure linear function. It takes as input the secret shares of feature $\langle x \rangle^A$ outputted from linear function, and outputs the secret shares of the normalized feature $\langle z \rangle^A$. We observe that its functionality given in Eq. 2 can be transformed to a simpler problem

$$z = \epsilon_1 \cdot x + \epsilon_2, \text{ where } \epsilon_1 = \frac{\gamma}{\delta}, \epsilon_2 = \beta - \frac{\gamma\mu}{\delta}. \quad (3)$$

Since $\epsilon_1, \epsilon_2$ are derived from the BN parameters and independent of inference input, they can be *pre-calculated* by model owner in the setup phase. With preprocessing, only Eq. 3 is required to be calculated. Such a conversion circumvents the complex division operations over secret shares in Eq. 2, resulting in a functionality more compatible to secret sharing techniques. With above observation, given the pre-generated shares of two parameters $\langle \epsilon_1 \rangle^A, \langle \epsilon_2 \rangle^A$, the $\mathsf{SBN}(\langle x \rangle^A, \langle \epsilon_1 \rangle^A, \langle \epsilon_2 \rangle^A)$ proceeds as follows: $S_0$ and $S_1$ jointly compute the normalized feature on each neuron $\langle z \rangle^A = \langle x \rangle^A \cdot \langle \epsilon_1 \rangle^A + \langle \epsilon_2 \rangle^A$.

### 4.4 Secure ReLU Function

The secure ReLU function (SReLU) is applied on each neuron and proceeds with the functionality $\mathsf{ReLU}(x) = max(x, 0)$ in the encrypted domain. Prior works that solve the problem is either relying on the heavyweight garbled circuit techniques [11], [19] or utilizing the linear activation functions (e.g., square function) [12], [13], [38]. In essence, the former requires intensive communication cost that is unsuitable for real-world mobile application deployment. Using a linear activation could be problematic and violates the original intention to apply activation function, i.e., introducing non-polynomiality. This is because an NN with all linear functions has limited power to handle complex inference problem (somewhat equivalent to linear regression) and makes the training process hard to converge during backpropagation [39].

**Overview.** In Sonic, we rely on a new highly efficient realization of the secure ReLU function in the secret sharing domain. We first note that with the fixed-point representation, the MSB indicating the sign bit of a non-negative

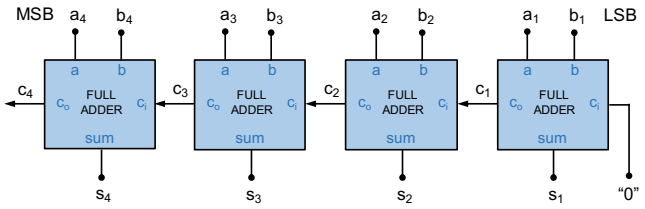


Fig. 6. An example of 4-bit ripple carry adder.

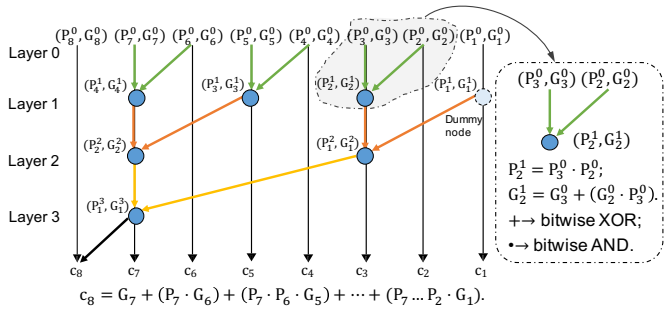


Fig. 7. An example of 8-bit parallel prefix adder.

feature $x$ would be 1 and a negative $x$ would be 0. We then transform the ReLU function into an MSB extraction via

$$max(x,0) \xrightarrow{\text{trans}} \neg\mathsf{MSB}(x)\cdot x = \begin{cases} 1\cdot x & \text{if } x \geq 0 \\ 0\cdot x & \text{if } x < 0 \end{cases}. \quad (4)$$

Based on Eq. 4, we decompose the SReLU function into four atomic operations. As summarized in Fig. 5, it comprises the *secure* MSB$(\cdot)$ *gadget*, the *secure NOT gadget*, the *secure* B2A$(\cdot)$ *gadget*, and the *secure multiplication gadget*. The *secure* MSB *gadget* takes as input the arithmetic shares of normalized feature $\langle x\rangle^A$, and extracts the boolean-shared MSB $[\![a_\ell]\!]$. The *secure NOT* conducts the bitwise-NOT to produce the shares of NOT MSB $[\![\bar{a}_\ell]\!]$.

Prior to multiplying with normalized feature $x$, the *secure* B2A *gadget* needs to be applied, converting the boolean shared NOT MSB $[\![\bar{a}_\ell]\!]$ to its arithmetic form $\langle\bar{a}_\ell\rangle^A$. The reason is that $[\![\bar{a}_\ell]\!]$ is projected to ring $\mathbb{Z}_2$ via $[\![\bar{a}_\ell]\!]_0 + [\![\bar{a}_\ell]\!]_1 \pmod 2$, whereas the arithmetic-shared feature $\langle x\rangle^A$ is projected to $\mathbb{Z}_{2^\ell}$ (via $\mathrm{mod}2^\ell$). These two shares cannot be naively multiplied with different moduli. The last *secure multiplication* produces the shares of ReLU result $\langle z\rangle^A$, given the shared NOT MSB and feature.

Below we expatiate on the essential cryptographic gadgets of secure ReLU function in Sonic: the *secure* MSB *gadget* and the *secure* BA2 *gadget*.

### 4.4.1 The Construction of Secure MSB Extraction

The secure MSB$(\cdot)$ gadget is used to securely extract the MSB of the arithmetic-shared data and to produce a boolean-shared MSB as the output. Suppose there are secret shares $\langle x\rangle_0^A$ and $\langle x\rangle_1^A$ of a secret value $x$, with the bit length $l$. Let $x = \{x_\ell, ..., x_1\}$, $a = \{a_\ell, ..., a_1\}$, and $b = \{b_\ell, ..., b_1\}$ denote $x, \langle x\rangle_0^A$, $\langle x\rangle_1^A$ with their corresponding bit strings respectively, such that $x = a + b \pmod{2^\ell}$. The key observation is that the difference between the sum $(+)$ of bit strings of $a, b$ and the bitwise-XOR $(\oplus)$ of the bit strings of $a, b$ is equal to the carry bits $c_\ell, \ldots, c_1$. For example, given $x = 13, a = 6, b = 7$, the carry bits ("0110") are equal to bit strings of $(a + b)$ ("1101") XOR with $a \oplus b$ ("1011"). Then extracting MSB $x_\ell = c_\ell + a_\ell + b_\ell$ is converted to calculating the carry bit $c_\ell$ via an $\ell$-bit full adder.

To do so, an effective and notable approach [16] is to use the ripple carry adder (RCA) to implement the $\ell$-bit full adder in serial. As Fig. 6 demonstrates, the fan-out carry bit $(c_o)$ of each full adder is propagated as fan-in $(c_i)$ of the succeeding full adder. This serial implementation introduces an $O(\ell)$ propagation delay, resulting in $2\ell$ rounds of communication (computing AND operations over boolean shares) between the two cloud servers in the secret sharing domain. The linear round complexity could result in long processing latency when the two cloud servers are geographically separated and the network delay is high.

Instead, we observe an efficient realization of full adder logic from the digital circuit design literature [40], called the parallel prefix adder (PPA). In comparison to RCA, the PPA can extract the MSB in logarithm communication rounds $\mathcal{O}(\log\ell)$. We note that leveraging parallel adder (the tree-based PPA and its other variants) to efficiently realize the secure MSB extraction has also been explored in independent and concurrent works [41], [42], [43], under different contexts.

The usage of the PPA for secure MSB extraction in Sonic is introduced as follows. In the PPA, a signal tuple $(G_i, P_i)$ can be pre-generated in parallel via

$$G_i = a_i \cdot b_i, P_i = a_i + b_i, \quad (5)$$

where $G_i$ is called the carry generate signal and $P_i$ is called the carry propagate signal. Given these two prefixes, PPA reformulates the full adder $c_{i+1} = (a_i \cdot b_i) + c_i \cdot (a_i + b_i)$ to compute the carry bit via $c_{i+1} = G_i + (c_i \cdot P_i)$. This reformulation allows a carry to be derived as follows:

$$c_\ell = G_{\ell-1} + (P_{\ell-1} \cdot G_{\ell-2}) + ... + (P_{\ell-1}...P_2 \cdot G_1), \quad (6)$$

without waiting for the previous carry propagated through all previous adders. Afterwards, PPA properly organizes the computation of Eq. 6 in parallel to reduce the latency in $O(\log\ell)$ rounds. As demonstrated in Fig. 7, PPA forms a $\log\ell$-layer binary tree and attaches a binary operator $\diamond$ on each node. This binary operator is defined as: given two carry generate signal and propagate signal tuples $(G_{in_1}, P_{in_1}); (G_{in_2}, P_{in_2})$, and output signal tuple $(G_{out}, P_{out})$, it performs

$$\begin{aligned} (G_{out}, P_{out}) &= (G_{in_1}, P_{in_1}) \diamond (G_{in_2}, P_{in_2}) \quad (7)\\ G_{out} &= G_{in_2} + G_{in_1} \cdot P_{in_2} \\ P_{out} &= P_{in_2} \cdot P_{in_1}. \end{aligned}$$

PPA recursively computes the above binary operation over the signal tuples at the leaf nodes (layer 0), and propagates the resulting tuples as input to the next layer's nodes, until reaching the root node (the node corresponding to tuple $(P_1^3, G_1^3)$ in Fig. 7). At the end, the most significant carry bit $c_\ell$ can be produced via Eq. 6 and the MSB is calculated by $x_\ell = c_\ell + a_\ell + b_\ell$. Based on above philosophy, the details of the secure MSB$(\cdot)$ gadget are presented in Fig. 8.

### 4.4.2 Secure B2A Gadget

The secure B2A gadget converts a boolean-shared data $[\![x]\!]$ into its arithmetic share $\langle x\rangle^A$. Given two cloud servers $S_0, S_1$, the secure B2A$([\![x]\!])$ gadget proceeds as follow:

1) $S_0$ sets two variables $\langle a\rangle_0^A = [\![x]\!]_0$, $\langle b\rangle_0^A = 0$;

**Input**: Arithmetic shares of integer feature $\langle x\rangle^A \in \mathbb{Z}_{2^\ell}$.
**Output**: Boolean shares of MSB $[\![x_\ell]\!] \in \mathbb{Z}_2$.
Decompose $x$ to bit strings:
1) $S_0$ decomposes $\langle x\rangle_0^A$ to a bit string $a_\ell, ..., a_1$;
   $S_1$ decomposes $\langle x\rangle_1^A$ to a bit string $b_\ell, ..., b_1$;
2) For each $k \in [1, \ell]$:
   $S_0$ sets $[\![a_k]\!]_0 = a_k$, $[\![b_k]\!]_0 = 0$, $[\![w_k]\!]_0 = a_k$;
   $S_1$ sets $[\![a_k]\!]_1 = 0$, $[\![b_k]\!]_1 = b_k$, $[\![w_k]\!]_1 = b_k$;
Compute signal tuples $(G, P)$ in Eq. 5:
3) For each $k \in [1, \ell]$:
   $S_0$ and $S_1$ set $[\![G_k]\!] = [\![a_k]\!] \cdot [\![b_k]\!]$, $[\![P_k]\!] = [\![a_k]\!] \oplus [\![b_k]\!]$;
Compute PPA tree based on Eq. 7:
4) **Layer** $L = 0$
   For $k \in [1, \ell]$, $S_i$ sets $([\![G_k^0]\!], [\![P_k^0]\!]) = ([\![G_k]\!], [\![P_k]\!])$.
5) **Layer** $L = 1$
   $S_i$ sets dummy node $([\![G_k^1]\!], [\![P_k^1]\!]) = ([\![G_k^0]\!], [\![P_k^0]\!])$;
   For $k \in [2, \ell/2]$:
   Let $in_1 = 2k - 2$, $in_2 = 2k - 1$;
   $([\![G_k^1]\!], [\![P_k^1]\!]) = ([\![G_{in_1}^0]\!], [\![P_{in_1}^0]\!]) \diamond ([\![G_{in_2}^0]\!], [\![P_{in_2}^0]\!])$;
6) **Layer** $L = 2, ..., \log \ell$
   For $k \in [1, \ell/2^L]$:
   Let $in_1 = 2k - 1$, $in_2 = 2k$;
   $([\![G_k^L]\!], [\![P_k^L]\!]) = ([\![G_{in_1}^{L-1}]\!], [\![P_{in_1}^{L-1}]\!]) \diamond ([\![G_{in_2}^{L-1}]\!], [\![P_{in_2}^{L-1}]\!])$;
Compute MSB:
7) $S_0$ and $S_1$ set $[\![c_\ell]\!] = [\![G_1^{\log \ell}]\!]$, $[\![x_\ell]\!] = [\![w_\ell]\!] + [\![c_\ell]\!]$;

Fig. 8. The secure MSB$(\cdot)$ gadget.

2) $S_1$ sets two variables $\langle a\rangle_1^A = 0$, $\langle b\rangle_1^A = [\![x]\!]_1$;
3) $S_0$ and $S_1$ set $\langle x\rangle^A = \langle a\rangle^A + \langle b\rangle^A - 2 \cdot \langle a\rangle^A \cdot \langle b\rangle^A$.

#### 4.4.3 Realization of Secure ReLU function

Given above secure MSB gadget and secure B2A gadget, and the arithmetic share of input feature $\langle x\rangle^A$, the secure ReLU function SReLU$(\langle x\rangle^A)$ proceeds as follows:

1) **Secure MSB extraction:** $S_0$ and $S_1$ run to get the MSB $[\![a_\ell]\!] \leftarrow$ MSB$(\langle x\rangle^A)$.
2) **Secure NOT:** $S_i$ sets the NOT MSB $[\![\bar{a}_\ell]\!] = [\![a_\ell]\!] + i$.
3) **Secure B2A:** $S_0$ and $S_1$ run to get the arithmetic-shared NOT MSB $\langle \bar{a}_\ell\rangle^A \leftarrow$ B2A$([\![\bar{a}_\ell]\!])$.
4) **Secure multiplication:** $S_0$ and $S_1$ set $\langle z\rangle^A = \langle \bar{a}_\ell\rangle^A \cdot \langle x\rangle^A$.

### 4.5 Secure Max Pooling Layer

The max pooling layer is used to down sample the features by choosing the maximum values within a certain sliding window. It is typically applied after the ReLU function. The secure max pooling layer (SMP) function in Sonicsecurely realizes the $\max(x_1, ..., x_n)$ functionality over secret shares. In particular, we transform the pairwise maximum operation into the secure comparison with MSB extraction based on Eq. 8 and a secure linear branching based on Eq. 9 via

$$b = \text{MSB}(a_1 - a_2) = \begin{cases} 0 & \text{if } a_1 \geq a_2 \\ 1 & \text{if } a_1 < a_2 \end{cases}; \tag{8}$$

$$\max(a_1, a_2) = (1 - b) \cdot a_1 + b \cdot a_2. \tag{9}$$

With above insights in mind, we provide the details of the SMP realization. Given the secure MSB$(\cdot)$ gadget and secure B2A$(\cdot)$ gadget, and the secret shares of input features within each max pooling window $\langle x_1\rangle^A, ..., \langle x_n\rangle^A$, the SMP$(\langle x_1\rangle^A, ..., \langle x_n\rangle^A)$ performs as follows:

1) For $k \in [1, n-1]$:
2) $S_i$ sets $\langle a_1\rangle_i^A = \langle x_k\rangle_i^A$, $\langle a_2\rangle_i^A = \langle x_{k+1}\rangle_i^A$.
3) **Secure comparison:** $S_0$ and $S_1$ run to get the comparison bit $[\![b]\!] \leftarrow$ MSB$(\langle a_1\rangle^A - \langle a_2\rangle^A)$.
4) **Secure B2A:** $S_0$ and $S_1$ run to get $\langle b\rangle^A \leftarrow$ B2A$([\![b]\!])$.
5) **Secure branching:** $S_0$ and $S_1$ set $\langle z\rangle^A = (i - \langle b\rangle^A) \cdot \langle a_1\rangle^A + \langle b\rangle^A \cdot \langle a_2\rangle^A$. $S_i$ sets $\langle x_{k+1}\rangle_i^A = \langle z\rangle_i^A$.

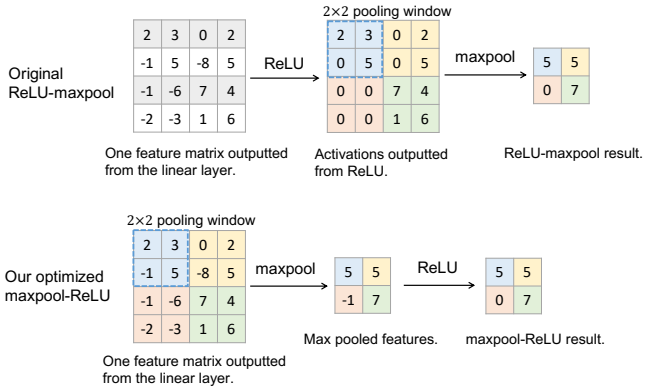


Fig. 9. An illustration of the optimized execution of ReLU and max pooling layer with typical $2 \times 2$ pooling window.

#### 4.5.1 Optimized Execution of ReLU and Max Pooling

We observe that reversing the execution order of ReLU and max pooling, i.e., maxpool(ReLU$(\cdot)$) $\rightarrow$ ReLU(maxpool$(\cdot)$) can greatly reduce the considerable workload to perform ReLU (75% saving on ReLU operations for a $2 \times 2$ max pooling window) [44]. This transformation is defined as

$$\begin{aligned} &\max(\max(x_1, 0), ..., \max(x_n, 0)) \\ &\xrightarrow{\text{transform}} \max(\max(x_1, ..., x_n), 0), \end{aligned}$$

where $x_1, ...x_n$ are the input features within the $n$-width pooling window. Such a conversion will reduce the number of secure comparison operations in the secret sharing domain and can significantly save the overall workloads. Because computing the non-polynomial ReLU over secret shares is knowingly complicated, the involved multiple interactions could lead to long processing latency.

Consider a typical max pooling layer with $2 \times 2$ pooling window. In principle, a max pooling layer is applied directly after the ReLU layer, where the 4 inputs within the $2 \times 2$ pooling window are the outputs of 4 ReLU operations. Then, it performs a series of comparisons as follows:

$$\begin{aligned} &\text{maxpool}(\text{ReLU}(x_1), \text{ReLU}(x_2), \text{ReLU}(x_3), \text{ReLU}(x_4)) \\ &= \max(\max(x_1, 0), \max(x_2, 0), \max(x_3, 0), \max(x_4, 0)). \end{aligned} \tag{10}$$

Since ReLU is monotonic (i.e., if $x_1 > x_2, \text{ReLU}(x_1) >= \text{ReLU}(x_2)$), the Eq. 10 is identical to

$$\begin{aligned} &\max(\max(x_1, x_2, x_3, x_4), 0) \\ &= \text{ReLU}(\text{maxpool}(x_1, x_2, x_3, x_4), 0), \end{aligned} \tag{11}$$

This article has been accepted for publication in a future issue of this journal, but has not been fully edited. Content may change prior to final publication. Citation information: DOI 10.1109/TDSC.2022.3141391, IEEE Transactions on Dependable and Secure Computing



where the internal maximum operation $\max(x_1, x_2, x_3, x_4)$ is regarded as the max pooling layer and the out-layer maximum operation $\max(\cdot, 0)$ is deemed as the ReLU activation. Through such a transformation, 75% of ReLU operations are saved given a typical max pooling with $2 \times 2$ window. A concrete illustration is given in Fig. 9

### 4.6 Complexity Analysis

We now provide an analysis of the complexity of Sonic's secure layer functions and secure gadgets regarding the number of communication rounds and the communication overhead. Table 2 summarizes the theoretical communication costs of non-linear layer functions (SReLU and SMP) and corresponding secure gadgets (secure MSB, secure B2A, and secure branching). We set the benchmark as the RCA based realization [16] for secure MSB. For SReLU and SMP, we set the benchmarks as the realizations based on RCA and GC [45], [46]. As defined, the bit length of an additive secret share is $\ell$, and the max pooling window size is $n$ (e.g., $n = 4$ if the pooling window is $2 \times 2$). Sonic's PPA based secure MSB gadget requires the communication as follows:

$$\begin{aligned} &4\ell + (\frac{\ell}{2} - 1) \cdot 8 + \frac{\ell}{2^2} \cdot 8 + ... + \frac{\ell}{2^{\log \ell}} \cdot 8 \\ =&4\ell - 8 + 8\ell \cdot (\frac{1}{2} + \frac{1}{2^2} + ... + \frac{1}{2^{\log \ell}}) \\ =&12\ell - 16 \end{aligned}$$

For the GC benchmarks, the communication costs are summarized based on the ReLU and max pooling circuits shown in prior work [45], [46] which consist of the secure conversions between additive shares to Yao's shares and corresponding ReLU and max pooling functionalities. Note that the GC protocols have constant round complexity $\mathcal{O}(1)$ as the concrete number of communication rounds depending on the specific realizations. As shown, Sonic's PPA based secure MSB, SReLU, and SMP have logarithmic round trip costs to the RCA based realizations with the same communication costs. Meanwhile, Sonic's SReLU and SMP substantially save the communication than the GC based realizations.

We also analyze the communication complexity of secure linear layers (SCONV, SFC and SBN) and corresponding secure gadget (SVDP) in Table 3. Suppose a typical stride is 1. Suppose the number of padding $p$, the sizes of input tensor, kernel, and output tensor of secure convolutional layer are $c^{in} \times n^{in} \times n^{in}$, $c^{in} \times c^{out} \times n \times n$, and $c^{out} \times n^{out} \times n^{out}$ respectively; and the sizes of input vector and output vector of the fully-connected layer are $c^{in}, c^{out}$, respectively.

TABLE 2
Communication Complexity Analysis of Secure Non-linear Layers

| Secure Function | Benchmarks | Communication | Round Complexity |
|---|---|---|---|
| Secure MSB | RCA | $12\ell - 16$ | $\mathcal{O}(\ell)$ |
| | Sonic | $12\ell - 16$ | $\mathcal{O}(\log \ell)$ |
| Secure B2A | Sonic | $4\ell$ | $\mathcal{O}(1)$ |
| Secure branching | Sonic | $8\ell$ | $\mathcal{O}(1)$ |
| SReLU | GC [45], [46] | $30\ell\kappa$ | $\mathcal{O}(1)$ |
| | RCA | $20\ell - 16$ | $\ell + 2$ |
| | Sonic | $20\ell - 16$ | $\log \ell + 2$ |
| SMP | GC [45], [46] | $(n+7)3\ell\kappa$ | $\mathcal{O}(1)$ |
| | RCA | $(n-1)(24\ell - 16)$ | $(n-1)(\ell + 2)$ |
| | Sonic | $(n-1)(24\ell - 16)$ | $(n-1)(\log \ell + 2)$ |

TABLE 3
Communication Complexity Analysis of Secure Linear Layers

| Secure Function | SVDP | SCONV | SFC | SBN |
|---|---|---|---|---|
| Comm. | $4\ell n$ | $c^{in}c^{out}(n^{in} - n + p + 1)^2 4\ell n$ | $c^{in}c^{out}4\ell n$ | $4\ell$ |
| # of Rounds | $n$ | $c^{out}(n^{in} - n + p + 1)^2 n$ | $c^{out}n$ | 1 |

## 5 Security Analysis

Sonic properly encrypts the user input, the CNN model (i.e., the weights), and any intermediate results as secret shares based on the standard secret sharing techniques [14], [47]. During Sonic's execution, the two non-colluding cloud servers receive only their corresponding secret shares that are uniformly distributed randomnesses and reveals nothing about private data. Each cloud proceeds Sonic's secure layer functions on its local shares independently. Any interactions between the two cloud servers are supported by the standard Beaver's triples [15] that can offer provably security guarantees on the exchanged secret shares.

Formally, we define an ideal functionality $\mathcal{F}_{\mathsf{ONI}}$ for securely proceeding an outsourced neural network inference protocol targeted in this paper. On top of this ideal functionality, we formally present the security definition and prove that Sonic's protocol $\Pi$ securely realizes this functionality in the ideal/real world simulation paradigm. We consider an adversary $\mathcal{A}$ to be semi-honest and can statically compromise the model owner, the mobile user, or anyone of the two cloud servers $S_0$, $S_1$ independently and so to capture the non-colluding property. In the ideal world, parties directly input and interact with the trusted functionality $\mathcal{F}_{\mathsf{ONI}}$ which executes the entire inference computation faithfully on behalf of the parties. In the real world, parties directly interact with Sonic's protocol $\Pi$ in the presence of above adversary $\mathcal{A}$. We say that protocol $\Pi$ securely realizes $\mathcal{F}_{\mathsf{ONI}}$ if for every adversary $\mathcal{A}$ from the real world execution of $\Pi$, there exists a probabilistic polynomial time (PPT) simulator $\mathcal{S}$ in the ideal world forging $\mathcal{A}$'s view such that $\mathcal{A}$ cannot distinguish the two scenarios.

We start with modeling the ideal functionality $\mathcal{F}_{\mathsf{ONI}}$.

***Definition 1.*** The ideal functionality $\mathcal{F}_{\mathsf{ONI}}$ of secure neural network inference outsourced to the cloud is modeled as follows:

- **Input.** The model owner $\mathcal{O}$ deploys the pre-trained CNN model $\mathbf{W}$ to $\mathcal{F}_{\mathsf{ONI}}$. The mobile user $\mathcal{U}$ submits the user input $\mathbf{X}$ to $\mathcal{F}_{\mathsf{ONI}}$. The two servers $S_0$ and $S_1$ inputs nothing to $\mathcal{F}_{\mathsf{ONI}}$.
- **Computation.** Upon receiving the model $\mathbf{W}$ from the model owner and the user input $\mathbf{X}$ from the mobile user, $\mathcal{F}_{\mathsf{ONI}}$ interacts in hybrid with the ideal functionalities of subroutines (i.e., layer-protocols) $\mathcal{F}_{\mathsf{SCONV}}$, $\mathcal{F}_{\mathsf{SBN}}$, $\mathcal{F}_{\mathsf{SReLU}}$, and $\mathcal{F}_{\mathsf{SMP}}$ to generate the prediction $\mathbf{z}$.
- **Output.** The $\mathcal{F}_{\mathsf{ONI}}$ outputs the prediction $\mathbf{z}$ to the mobile user and nothing to the model owner.

We define the security guarantees.

***Definition 2.*** Protocol $\Pi$ is said to securely evaluate the functionality $\mathcal{F}_{\mathsf{ONI}}$ in the presence of semi-honest adversaries in a static corruption, if for every PPT adversary $\mathcal{A}$ for

This article has been accepted for publication in a future issue of this journal, but has not been fully edited. Content may change prior to final publication. Citation information: DOI 10.1109/TDSC.2022.3141391, IEEE Transactions on Dependable and Secure Computing



the real model, there exits a PPT simulator $\mathcal{S}$ for the ideal model, such that for every party $\mathcal{P} \subset [\mathcal{O}, \mathcal{U}, S_0, S_1]$

$$\{\text{IDEAL}_{\mathcal{F}_{\mathsf{ONI}},\mathcal{P},\mathcal{S}(\bar{X})}(\mathbf{X},\mathbf{W})\}_{\mathbf{X},\mathbf{W},\bar{X}} \stackrel{c}{\equiv} \{\text{REAL}_{\Pi,\mathcal{P},\mathcal{A}(\bar{X})}(\mathbf{X},\mathbf{W})\}_{\mathbf{X},\mathbf{W},\bar{X}}.$$

where $\text{IDEAL}_{\mathcal{F}_{\mathsf{ONI}},\mathcal{P},\mathcal{S}(\bar{X})}(\mathbf{X},\mathbf{W})$ is the output of joint execution of $\mathcal{F}_{\mathsf{ONI}}$ in the ideal world, $\text{REAL}_{\Pi,\mathcal{P},\mathcal{S}(\bar{X})}(\mathbf{X},\mathbf{W})$ is the output of and $\bar{X}$ denotes the auxiliary input. We consider the following cases:

- **Corrupted model owner.** A corrupted model owner is required to learn no private information about the values of user input $\mathbf{X}$. In this case, there should have a simulator $\mathcal{S}$ that interacts with $\mathcal{O}$ and extracts the model inputted from $\mathcal{A}$ to honest parties $S_0, S_1$. $\mathcal{O}$ cannot distinguish from the transcripts whether interacting with $\mathcal{S}$ from the ideal execution of $\mathcal{F}_{\mathsf{ONI}}$ or from the real execution of $\Pi$.
- **Corrupted mobile user.** A corrupted mobile user is required to learn no private information about the values of model weights and coefficients $\mathbf{W}$ beyond the hyper-parameters made public available. In this case, there should have a simulator $\mathcal{S}$ that interacts with $\mathcal{U}$, extracts the user input $\mathbf{X}$ inputted from $\mathcal{U}$ to honest parties $S_0, S_1$, and emulates the output $\mathbf{z}$. The corrupted mobile user $\mathcal{U}$ cannot distinguish from the transcripts whether interacting with $\mathcal{S}$ from the ideal execution of $\mathcal{F}_{\mathsf{ONI}}$ or from the real execution of $\Pi$.
- **Corrupted cloud server.** A corrupted cloud server $S_i \in [S_0, S_1]$ is required to learn no private information about the values of user input $\mathbf{X}$, model weights and coefficients $\mathbf{W}$ beyond the hyper-parameters. In this case, there should has a simulator $\mathcal{S}$ that interacts with the corrupted $S_i$ and emulates the exact transcripts for interactions between the adversary $S_i$ and honest parties $\mathcal{O}, \mathcal{U}, S_{1-i}$. The corrupted cloud server $S_i$ cannot distinguish from the transcripts whether interacting with $\mathcal{S}$ from the ideal execution of $\mathcal{F}_{\mathsf{ONI}}$ or from the real execution of $\Pi$.

***Theorem 1.*** Sonic's protocol $\Pi$ securely realizes $\mathcal{F}_{\mathsf{ONI}}$ (per Definition 2) in the presence of one semi-honest adversary $\mathcal{A}$ in the ($\mathcal{F}_{\mathsf{SCONV}}$, $\mathcal{F}_{\mathsf{SBN}}$, $\mathcal{F}_{\mathsf{SReLU}}$, $\mathcal{F}_{\mathsf{SMP}}$)-hybrid model.

***Proof 1.*** We begin by defining the simulator $\mathcal{S}$ based on the corrupted party. The simulator should be able to emulate the transcripts (including the joint distribution of the inputs and outputs) that are computationally indistinguishable from the ones in ideal world execution. That is, the transcripts during real interaction are exactly simulated and the honest parties should learn the correct outputs. In the hybrid argument, the executions of the subroutines (layer-protocols) are simulated by $\mathcal{S}$ which plays the roles of honest parties in corresponding ideal functionalities. We construct $\mathcal{S}$ for the following corruption parties:

- **Simulator for the corrupted model owner.** The only work where the corrupted model owner $\mathcal{O}$ engaged in protocol $\Pi$ is inputting the secret-shared NN model $\mathbf{W}$. The simulator $\mathcal{S}$ plays the role of the corrupted model owner $\mathcal{O}$ in the ideal world by submitting the model $\mathbf{W}$ of $\mathcal{O}$ to the ideal functionality $\mathcal{F}_{\mathsf{ONI}}$. The remaining protocol $\Pi$ runs by the honest two cloud servers by sequentially composing the ideal functionalities of subroutines. At the end of $\Pi$, only the shares of correct result $\mathbf{z}$ is returned to the honest mobile user $\mathcal{U}$ so to achieve the correctness, and nothing is outputted to $\mathcal{O}$. To emulate the view of $\mathcal{O}$, the simulator $\mathcal{S}$ simply outputs the model $\mathbf{W}$ in a dummy way. The $\mathcal{S}$'s output (i.e., $\mathcal{S}(\mathbf{W})$) is identically distributed to the view of $\mathcal{O}$ (i.e., $\text{View}_{\mathcal{U}}^{\Pi}(\mathbf{W})$), and thus the real and ideal worlds are indistinguishable.
- **Simulator for the corrupted mobile user.** The corrupted mobile user $\mathcal{U}$ engages in protocol $\Pi$ by submitting the secret shares of user input $\mathbf{X}$, and receives the two shares $\langle \mathbf{z} \rangle_0, \langle \mathbf{z} \rangle_1$ of inference result $\mathbf{z}$. The simulator $\mathcal{S}$ plays the role of the corrupted mobile user $\mathcal{U}$ in the ideal world by submitting the user input $\mathbf{X}$ to $\mathcal{F}_{\mathsf{ONI}}$. Upon receiving the inference result $\mathbf{z}$ from $\mathcal{F}_{\mathsf{ONI}}$, $\mathcal{S}$ generates a random value as $\langle \mathbf{z}^* \rangle_0 \in_R \mathbb{Z}_{2^\ell}$ and computes $\langle \mathbf{z}^* \rangle_1 = \mathbf{z} - \langle \mathbf{z}^* \rangle_0$. Then $\mathcal{S}$ outputs $\langle \mathbf{z}^* \rangle_0, \langle \mathbf{z}^* \rangle_1$. The security follows from the fact that the additive secret shares $\langle \mathbf{z}^* \rangle_0, \langle \mathbf{z}^* \rangle_1$ are uniformly random values in $\mathbb{Z}_{2^\ell}$, and are identically distributed to the transcripts from real world. Meanwhile, the result $\mathbf{z}$ can be reconstructed via $\langle \mathbf{z}^* \rangle_0 + \langle \mathbf{z}^* \rangle_1 \pmod{2^\ell}$. The output $\mathcal{S}(\mathbf{X}, \mathbf{z})$ and the view of $\mathcal{U}$ (i.e., $\text{View}_{\mathcal{U}}^{\Pi}(\mathbf{X}, \mathbf{z})$) are identically distributed, and thus the two worlds are thus indistinguishable.
- **Simulator for a corrupted cloud server.** The two cloud servers $S_0$ and $S_1$ jointly proceed protocol $\Pi$ in a symmetric way without submitting any inputs and receiving the final result. That is, they compute and interact with each other over all secret shares in different layers of $\Pi$. Given their symmetry, it is sufficient to construct a simulator $\mathcal{S}$ for one of the server, say $S_0$. In the subsequent protocol, $\mathcal{S}$ sequentially composes the simulators of subroutines, which play the role of honest cloud server $S_1$ to interact with $S_0$. All messages involved in the subroutines are random shares of matrices with the dimensions are consistent to the honest server's shares. The interactions between two servers are simulated by the simulator $\mathcal{S}_{\mathsf{BTri}}$ for the functionality of Beaver's multiplication $\mathcal{F}_{\mathsf{BTri}}$, which interacts with $S_0$ over random shares. The security follows from the fact that all transcripts are uniformly distributed secret shares that can be emulated with random values in $\mathbb{Z}_{2^\ell}$, and the view of $S_0$ in every interaction in $\Pi$ is indistinguishable from the view emulated by $\mathcal{S}_{\mathsf{BTri}}$. Hence, we argue that $\mathcal{S}$ in the hybrid model can emulate the view of $S_0$, and thus the two worlds are indistinguishable. The above concludes the proof of Theorem 1.

TABLE 4
Time and Bandwidth of Atomic Layer Functions

| | SCONV $3\times3$ | SCONV $5\times5$ | SBN | SReLU | SMP $2\times2$ |
|---|---|---|---|---|---|
| Time (ms) | 5.04 | 7.07 | 15.35 | 22.3 | 43.1 |
| Comm. (KB) | 0.14 | 0.39 | 0.016 | 0.03 | 0.14 |

## 6 Performance Evaluation

### 6.1 System Implementation

We implement a prototype of Sonic in Java. Evaluations are executed on two servers, running CentOS 7 and equipped

This article has been accepted for publication in a future issue of this journal, but has not been fully edited. Content may change prior to final publication. Citation information: DOI 10.1109/TDSC.2022.3141391, IEEE Transactions on Dependable and Secure Computing



TABLE 5
Time and Bandwidth of the SFC Layer

| Layer Size ($n \times n$) | 64 | 128 | 256 | 512 | 1024 |
|---|---|---|---|---|---|
| Time (ms) | 0.12 | 0.19 | 0.234 | 0.35 | 0.65 |
| Comm. (MB) | 0.16 | 0.42 | 1.24 | 4.46 | 17.33 |

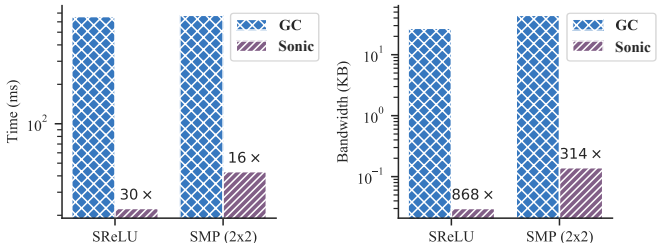


Fig. 10. Time and bandwidth comparison of the SReLU and SMP layers.

with Intel Xeon Gold 6150 CPU @2.7GHz processor, 192GB RAM, Mellanox Spectrum network. The reported measurements use the MNIST and CIFAR-10 machine learning benchmarking datasets with four CNNs, where M1, M2 are trained on MNIST and C1, C2 are trained on CIFAR-10. We refer the readers to Sec. 6.6 for the details of the model architectures. Consistent with prior art [11], [24], we evaluate the benchmarks in the LAN setting.

Sonic's secure NN inference works in the secret sharing domain, where all data are represented in fixed-point integers and shared over ring $\mathbb{Z}_{2^\ell}$. In essence, we set the ring size as $\mathbb{Z}_{2^{32}}$. This setting of ring is consistent with prior work [13]. To present the weights to 32-bit fixed-point integers, we set the scaling factor $q$ as 1024, 128, 64, and 128 for M1, M2, C1, and C2, respectively. Our implementation can further seamlessly support the 64-bit ring $\mathbb{Z}_{2^{64}}$, where this choice of ring size enables us to losslessly embed more deep and complex NNs, like the C1 and C2 for CIFAR-10. We provide varying the ring size of C1 and C2 to $\mathbb{Z}_{2^{64}}$ with the factors 65536 and 131070, and report corresponding experiment results.

We implement the training procedure based on PyTorch backend and train the models over plaintext datasets on NVIDIA Tesla V100 GPU. All four networks are trained with standard SGD optimizer is adapted with cosine learning rate decay, and we set the training parameters as the initial learning rate 0.1, batch size 256, momentum 0.9, and the weight decay $5 \times 10^{-4}$ for every 50 epochs. For both MNIST and CIFAR-10, all images are scaled to integers in $[0, 255]$. In this way, all user input images can be directly supplied to Sonic's secure inference without data preprocessing.

### 6.2 Microbenchmarks

**Secure layer functions.** We benchmark the performance of secure layer functions as the building blocks used for Sonic's secure inference. Table 4 summarizes the time and bandwidth consumptions of each layer function. For demonstration, we choose the commonly-used kernel sizes $3 \times 3$ and $5 \times 5$ for the SCONV layer, and $2 \times 2$ pooling window for the SMP layer. As shown, all functions can be accomplished within 50ms and require less than 0.5KB bandwidth regardless the window size. Table 5 depicts the

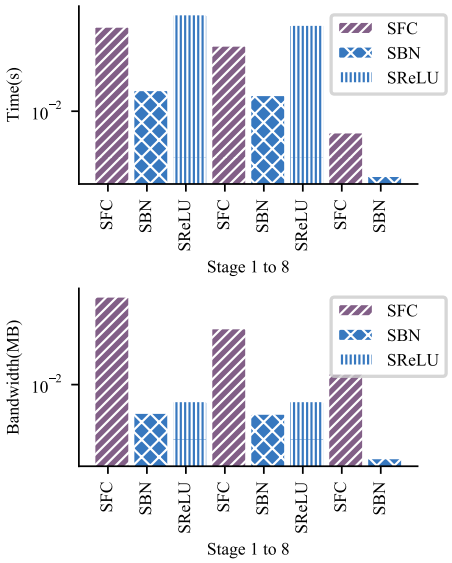


Fig. 11. Performance breakdown of M1. Left: time; Right: bandwidth.

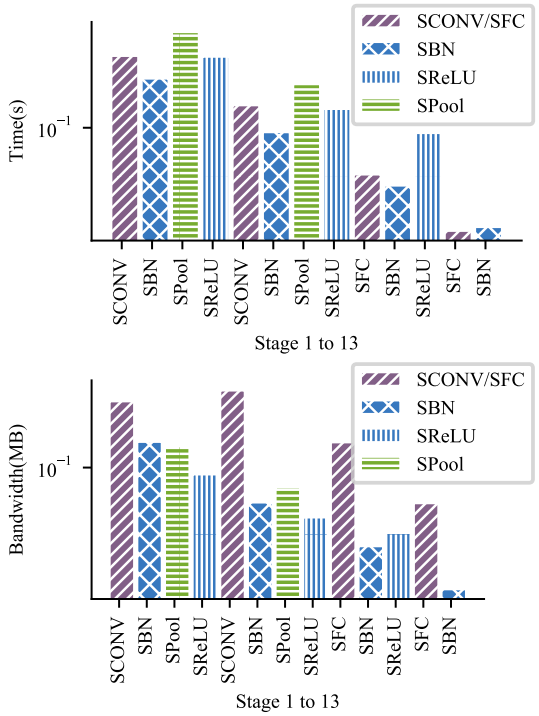


Fig. 12. Performance breakdown of M2. Top: time; Bottom: bandwidth.

performance of the SFC layer over a series of $n \times n$ layers, i.e., both input and output layers are with $n$ neurons. With the growth of $n$, the time (left figure) increases linearly attributed to our batch processing, and the bandwidth (right figure) ascends quadratically.

**ReLU and MaxPool comparison with GC.** Fig. 10 demonstrates the performance improvements for Sonic's SReLU and SMP functions over a baseline realized based on GC. The GC baseline realizes equivalent functionalities to Sonic, is implemented on FlexSC with the free-XOR and half-AND optimizations. Compared with the GC baseline, Sonic requires $30\times$ lower latency and $868\times$ less communication for the SReLU function. Besides, Sonic saves $16\times$ latency and

This article has been accepted for publication in a future issue of this journal, but has not been fully edited. Content may change prior to final publication. Citation information: DOI 10.1109/TDSC.2022.3141391, IEEE Transactions on Dependable and Secure Computing



TABLE 6
Performance Summary of the Benchmarking Models with 32-bit Implementation

| Dataset | Model | Cloud Time (s) | Cloud Comm. (MB) | Mobile User [a] Time (ms) | Model Owner [b] Time (s) | Layers |
|---|---|---|---|---|---|---|
| MNIST | M1 | 0.7 | 1.8 | 0.5 | 0.02 | 3SFC + SBN + SBA |
| | M2 | 13.6 | 10.8 | 0.7 | 0.11 | 4SCONV/SFC + SBN + SBA, 2SMP |
| CIFAR-10 | C1 | 161.2 | 711.4 | 2.5 | 5.9 | 8SCONV/SFC + SBN + SBA, 2SMP |
| | C2 | 94.7 | 186.9 | 2.4 | 1.6 | 10SCONV/SFC + SBN + SBA, 3SMP |

[a] Cost of generating shares of an image during preprocessing.
[b] One-time cost of generating shares of the model during preprocessing.

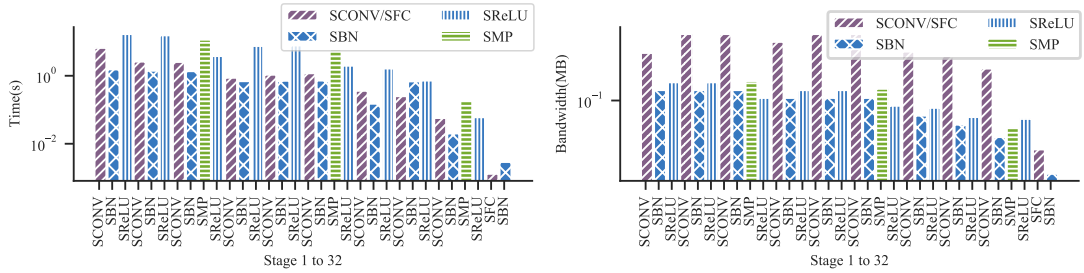


Fig. 13. Performance breakdown of C1. Left: time; Right: bandwidth.

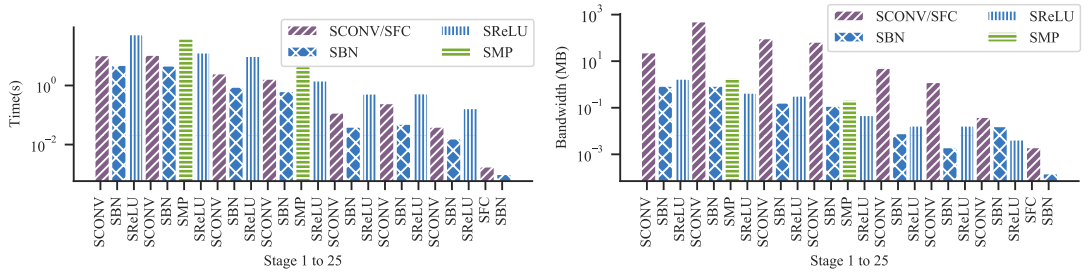


Fig. 14. Performance breakdown of C2. Left: time; Right: bandwidth.

TABLE 7
Performance Summary of the 64-bit Implementation of Models on CIFAR-10

| Model | Cloud Time (s) | Cloud Comm. (MB) | Mobile User [a] Time (ms) | Model Owner [b] Time (s) |
|---|---|---|---|---|
| C1 | 227.0 | 1239.5 | 9.0 | 14.06 |
| C2 | 123.1 | 373.7 | 9.6 | 5.86 |

[a] Cost of generating shares of an image during preprocessing.
[b] One-time cost of generating shares of the model.

TABLE 8
Summary of Inference Accuracy

| MNIST | | | CIFAR-10 | | | |
|---|---|---|---|---|---|---|
| Model | Sonic | Plaintext | Model | Sonic 32-bit | Sonic 64-bit | Plaintext |
| M1 | 97.0% | 97.0% | C1 | 75.0% | 84.0% | 80.9% |
| M2 | 99.12% | 99.12% | C2 | 80.0% | 88.0% | 81% |

$314\times$ communication cost for the SMP function. The reported results show that our proposed secret sharing based designs are more lightweight and applicable for practical requirements, compared with the prior constructions relying on GC [12], [19], [20], [24].

### 6.3 Sonic's Protocol

**Evaluation over ring $\mathbb{Z}_{2^{32}}$.** We evaluate Sonic's secure NN inference protocol on four models over machine learning benchmarking datasets MNIST and CIFAT-10. Table 6 summarizes Sonic's overall performance running at the cloud. The models M1 with 3(FC-BN-ReLU) and M2 with 4(CONV/FC-BN-ReLU)-2MP for MNIST dataset are relatively simple. Sonic performs high-quality predictions (97% for M1, 99% for M2) with 0.7s and 13.6s online processing time. The models C1 and C2 are trained for CIFAR-10. C1 adapts the MiniONN architecture [11] with 8(CONV/FC-BN-ReLU)-2MP, which is commonly evaluated in prior secure NN inference works. C2's architecture is in line with the FitNet [48] with 10(CONV/FC-BN-ReLU)-3MP. For the more complex C1 and C2, Sonic's predictions require 2.68min and 1.58min respectively. The workloads on the mobile user (within 2.5ms) and model owner (within 6s) sides are light, which confirms that Sonic is suitable for end-users with resource constrained devices. Note that the workload at the model owner side is one-time cost and determined by the NN's size.

We further report the performance breakdown of each network to have a more comprehensive understanding of resource consumptions. As shown in Fig. 11, Fig. 12, Fig. 13 and Fig. 14, the time (left/top figures) and bandwidth (right/bottom figures) costs for each stage in M1 (8 stages) and M2 (10 stages) on MNIST dataset, C1 (32 stages) and C2

This article has been accepted for publication in a future issue of this journal, but has not been fully edited. Content may change prior to final publication. Citation information: DOI 10.1109/TDSC.2022.3141391, IEEE Transactions on Dependable and Secure Computing



TABLE 9
Bandwidth Comparison of Sonic with Prior Art on MNIST

| Model | Prior Art | Bandwidth (MB) |
|---|---|---|
| M1 | MiniONN [11] | 15.8 |
| | Chameleon [17] | 10.5 |
| | EzPC [49] | 70 |
| | Gazelle (approx.) [12] | 0.5 |
| | XONN (trimmed BNN) [24] | 4.29 |
| | **Sonic (our design)** | **1.8** |
| M2 | MiniONN [11] | 657.5 |
| | EzPC [49] | 501 |
| | Gazelle (ReLU) [12] | 70 |
| | XONN (trimmed BNN) [24] | 32.13 |
| | **Sonic (our design)** | **10.8** |

TABLE 10
Bandwidth Comparison of Sonic's 32-bit and 64-bit Implementations with Prior Art on CIFAR10

| Model | Prior Art | Bandwidth (MB) |
|---|---|---|
| C1 | MiniONN [11] | 9272 |
| | Chameleon [17] | 2650 |
| | EzPC [49] | 40683 |
| | Gazelle (approx.) [12] | 1236 |
| | Gazelle (ReLU) [12] | ∼5000 |
| | XONN-1 [24] | 1290 |
| | XONN-2 [24] | 5099 |
| | **Sonic (32-bit ring)** | **711** |
| | **Sonic (64-bit ring)** | **1239.5** |
| C2 | XONN-1 [24] | 2599 |
| | XONN-2 [24] | 3461 |
| | **Sonic (32-bit ring)** | **186.9** |
| | **Sonic (64-bit ring)** | **373.7** |

(25 stages) on CIFAR10 dataset, respectively. As seen, the linear layers occupy most of network resources, and non-polynomial functions usually require more computation.

**Evaluation over ring $\mathbb{Z}_{2^{64}}$.** As above mentioned, Sonic provides a 64-bit implementation to support complex and deeper networks. We evaluate Sonic with such choice of ring size on CIFAR-10 and benchmark the results in Table 7. For the models C1 and C2, Sonic performs the secure inference with 3.7min and 2.05min computational time, and 1239MB and 373MB bandwidth costs, respectively. The workloads of the mobile user (within 10ms) and the model owner (within 15s) are lightweight. We note that enlarging the ring size increases their costs. This is because that our prototype is implemented in Java, the 64-bit numbers exceed the primitive data type (i.e., long), and the modular operations needs to work over costly BigInteger data type.

### 6.4 Summary of Accuracy

We report the Sonic's prediction accuracy by varying the ring sizes and compare the results with corresponding plaintext predictions in Table 8. As shown, Sonic's secure inference of the M1 and M2 models on MNIST achieves the same accuracy with plaintext predictions, i.e., 97% and 99% accurate predictions respectively. For CIFAR-10, Sonic varies the ring sizes. For the C1 and C2 over 32-bit ring, Sonic produces 75% and 80% accurate inference results, a slight and reasonable lower than the plaintext predictions accuracy 80.9% and 81%. For the C1 and C2 over 64-bit ring, Sonic's inference achieves high-quality results with 84% and 88% accuracy. Such results are more accurate than corresponding plaintext predictions, as the quantization of model weights prevent the overfitting of models. We are aware a tension in between the efficiency and utility in Sonic, i.e., the 64-bit implementation produces more accurate predictions than the 32-bit one yet trading with additional computational and bandwidth overheads.

TABLE 11
Time Comparison of Sonic with Prior Art on CNNs over MNIST

| Model | Prior Art | Time (s) | Implementation, Deployment |
|---|---|---|---|
| M1 | SecureML [19] | 4.88 | C++, outsourced |
| | MiniONN [11] | 1.04 | C++, interactive |
| | Chameleon [17] | 2.24 | C++, 3PC |
| | EzPC [49] | 0.7 | C++, outsourced |
| | **Sonic (our design)** | **0.7** | Java, outsourced |
| M2 | CryptoNets [38] | 297.5 | C++, interactive |
| | MiniONN [11] | 9.32 | C++, interactive |
| | EzPC [49] | 14.5 | C++, outsourced |
| | Gazelle (ReLU) [12] | 1.37 | C++, interactive |
| | **Sonic (our design)** | **13.6** | Java, outsourced |

TABLE 12
Time Comparison of Sonic with Prior Art on CNNs over CIFAR-10

| Prior Art | Time (s) | Implementation, Deployment |
|---|---|---|
| MiniONN [11] | 544 | C++, interactive |
| Chameleon [17] | 52.67 | C++, 3PC |
| EzPC [49] | 265.6 | C++, outsourced |
| Gazelle (ReLU) [12] | 140 | C++, interactive |
| **Sonic (our design)** | **94.7** | Java, outsourced |

### 6.5 Comparison with Prior Art

To demonstrate Sonic practical and lightweight, we compare Sonic's bandwidth with notable prior secure NN inference systems. All measurements are reported from their papers, and the cost of Gazelle with all-ReLU activations is given in Delphi. Table 9 and Table 10 summarize the bandwidth costs on MNIST and CIFAR10 corresponding to each model. For MNIST, Sonic achieves up to $38\times$ and $60\times$ bandwidth savings over M1 and M2 compared with prior art except for Gazelle with the polynomial approximated activation. However, as aforementioned, Gazelle's client-server protocol aggravates the workload on client, including the homomorphic encryption/decryption and interactions with the model owner.

Table 10 compares Sonic's bandwidth costs over 32-bit and 64-bit ring sizes with prior art on CIFAR-10 dataset. All results are directly employed from their papers, while the cost of Gazelle with ReLU is reported in Delphi. For XONN, it applies network trimming techniques and enlarges the model with some scaling factor to increase the accuracy. This technique results in different accuracy and bandwidth for the same NN model, depending on the portion of neurons pruned off and the scaling factor.

For the model C1, XONN-1 requires 1290MB bandwidth with 72% accuracy and XONN-2 requires 5099MB bandwidth with 80% accuracy. Sonic's 32-bit and 64-bit implementations achieves 75%, 84% accurate predictions with 711MB, 1239.5MB bandwidth, amounting to $1.8\times$, $4.1\times$ lower costs and higher accuracy than XONN-1 and XONN-2, respectively. Compared with other works, Sonic's 32-bit

This article has been accepted for publication in a future issue of this journal, but has not been fully edited. Content may change prior to final publication. Citation information: DOI 10.1109/TDSC.2022.3141391, IEEE Transactions on Dependable and Secure Computing



implementation requires the least bandwidth costs. Sonic's 64-bit implementation achieves a 7.5×, 2×, 32.8×, 4× bandwidth savings compared with MiniONN, Chameleon, EzPC, and Gazelle with all ReLU activations, respectively.

For the model C2, XONN-1 consumes 2599MB bandwidth with 81% accuracy and XONN-2 consumes 3461MB bandwidth with 84% accuracy. Sonic's 32-bit and 64-bit implementations cost 186.9MB, 373.7MB bandwidth with 75%, 84% accurate predictions, resulting in 13.9×, 9.3× savings and higher quality compared with XONN-1 and XONN-2, respectively. We note that Delphi [13] introduces an optimization on network architecture to improve the performance while preserving satisfactory accuracy. It trains a series of models with different architectures by replacing different portion of ReLU activations with polynomial approximations under tuned coefficients. However, this optimization has uncertainty in practice, as such process requires extra training costs which could be time-consuming [50].

Table 11 and Table 12 summarize the computational costs on the Convolutional NNs over MNIST and CIFAR-10 datasets. As shown, for the model M1, Sonic achieves 6.9×, 1.48×, 3.2× speedup over SecureML, MiniONN, Chameleon, respectively, and the time cost of Sonic is comparable to EzPC. In addition, for the model M2, Sonic is 21.8× and 1.1× faster than CryptoNets and EzPC, and the time cost of Sonic is comparable to MiniONN. For CIFAR-10, Sonic demonstrates 5.7×, 2.8×, 1.4× faster secure inference than the MiniONN, EzPC, and Gazelle, respectively. We are aware that some of prior works achieves better inference time than Sonic. However, we emphasize that the time comparison is not a fair comparison due to the following two-fold reasons. From the implementation perspective, most prior works are implemented in C++ whereas Sonic is implemented in Java. It is known that the computational performance of C++ programs are a few orders of magnitudes better than Java based programs. For example, Gazelle is implemented in C++ with SIDM optimization and is running on more powerful computers with faster CPU than Sonic. Moreover, some of the prior systems consider the client-server deployment scenario, where the private model weights and the client input are hidden from the counterparty. The secure protocols of these systems *do not need* to work over encrypted model and the encrypted input at the same time. In comparison, the secure outsourced inference systems (including Sonic, SecureML) require to ensure the security of the model and the client input *simultaneously*, i.e., the secure protocols are executed over both encrypted model weights and the encrypted client input. Some other works require multiple servers that increase the deployment overhead than the two-server model, for example, the offline phase in Chameleon is designed under the three-server setting.

### 6.6 Model Architectures

This section presents the details of model architectures used in our evaluation. For MNIST, the model M1 (summarized in Table 13) is comprised of 3 fully-connected (FC) layers, each of the FC layer is followed by the batch normalization (BN) and ReLU. It has been used in prior works [11], [12], [17], [19], [24], [49]. The model M2 (reported in Table 14) has been used in prior works [11], [12], [24], [49], which consists of 3 convolutional layers followed by BN and ReLU, 2 max pooling (MP) layers and 1 FC. For CIFAR-10, we use two more complex models C1 and C2. The model C1 (reported in Table 15) has been used in prior works [11], [12], [17], [24] for a benchmarking evaluation, which consists of 7 CONV layers followed by BN and ReLU, 2 MP layers and 1 FC layer. The model C2 (reported in Table 16) is a variant of FitNets (a thin deep network) and has been adopted in the XONN [24] with its trimmed binarized version, which consists of 9 CONV layers followed by BN and ReLU, 3 MP layers and 1 FC layer.

TABLE 13
Model Architecture of M1

| Layer | # SVDP | Padding, Stride |
|---|---|---|
| FC (784 → 128) - BN - ReLU | 128 | NA, NA |
| FC (128 → 128) - BN - ReLU | 128 | NA, NA |
| FC (128 → 10) - BN | 10 | NA, NA |

TABLE 14
Model Architecture of M2

| Layer | # SVDP | Padding, Stride |
|---|---|---|
| CONV (input: $\mathbb{R}^{1\times28\times28}$, kernel: $\mathbb{R}^{1\times16\times5\times5} \rightarrow \mathbb{R}^{16\times24\times24}$) - BN - ReLU | 1×9216 | NA, 1 |
| MP (input: $\mathbb{R}^{16\times24\times24}$, window: $\mathbb{R}^{16\times2\times2} \rightarrow \mathbb{R}^{16\times12\times12}$) | NA | NA, 2 |
| CONV (input: $\mathbb{R}^{16\times12\times12}$, kernel: $\mathbb{R}^{16\times16\times5\times5} \rightarrow \mathbb{R}^{16\times8\times8}$) - BN - ReLU | 16×1024 | NA, 1 |
| MP (input: $\mathbb{R}^{16\times8\times8}$, window: $\mathbb{R}^{16\times2\times2} \rightarrow \mathbb{R}^{16\times4\times4}$) - BN - ReLU | NA | NA, 2 |
| FC (256 → 100) - BN - ReLU | 100 | NA, NA |
| FC (100 → 10) - BN | 10 | NA, NA |

TABLE 15
Model Architecture of C1

| Layer | # SVDP | Padding, Stride |
|---|---|---|
| CONV (input: $\mathbb{R}^{3\times32\times32}$, kernel: $\mathbb{R}^{3\times64\times3\times3} \rightarrow \mathbb{R}^{64\times30\times30}$) - BN - ReLU | 3×57600 | NA, 1 |
| CONV (input: $\mathbb{R}^{64\times30\times30}$, kernel: $\mathbb{R}^{64\times64\times3\times3} \rightarrow \mathbb{R}^{64\times28\times28}$) - BN - ReLU | 64×50176 | NA, 1 |
| MP (input: $\mathbb{R}^{64\times28\times28}$, window: $\mathbb{R}^{64\times2\times2} \rightarrow \mathbb{R}^{64\times14\times14}$) | NA | NA, 2 |
| CONV (input: $\mathbb{R}^{64\times14\times14}$, kernel: $\mathbb{R}^{64\times64\times3\times3}$, feature: $\mathbb{R}^{64\times12\times12}$) - BN - ReLU | 64×9216 | NA, 1 |
| CONV (input: $\mathbb{R}^{64\times12\times12}$, kernel: $\mathbb{R}^{64\times64\times3\times3} \rightarrow \mathbb{R}^{64\times10\times10}$) - BN - ReLU | 64×6400 | NA, 1 |
| MP (input: $\mathbb{R}^{64\times10\times10}$, window: $\mathbb{R}^{64\times2\times2} \rightarrow \mathbb{R}^{64\times5\times5}$) | NA | NA, 2 |
| CONV (input: $\mathbb{R}^{64\times5\times5}$, kernel: $\mathbb{R}^{64\times64\times3\times3} \rightarrow \mathbb{R}^{64\times3\times3}$) - BN - ReLU | 64×576 | NA, 1 |
| CONV (input: $\mathbb{R}^{64\times3\times3}$, kernel: $\mathbb{R}^{64\times64\times3\times3} \rightarrow \mathbb{R}^{64\times3\times3}$) - BN - ReLU | 64×576 | 0, 1 |
| CONV (input: $\mathbb{R}^{64\times3\times3}$, kernel: $\mathbb{R}^{16\times64\times3\times3} \rightarrow \mathbb{R}^{16\times3\times3}$) - BN - ReLU | 64×144 | 0, 1 |
| FC (144 → 10) - BN | 10 | NA, NA |

## 7 Related Works

### 7.1 Secure Neural Network Inference

Secure neural network inference has received increasing attention in recent years. Most of prior works [11], [12], [13], [24], [38], [39], [41], [51] consider a scenario where

TABLE 16
Model Architecture of C2

| Layer | # SVDP | Padding, Stride |
|---|---|---|
| CONV (input: $\mathbb{R}^{3\times32\times32}$, kernel: $\mathbb{R}^{3\times16\times3\times3} \rightarrow \mathbb{R}^{16\times32\times32}$) - BN - ReLU | 3×16384 | 0, 1 |
| CONV (input: $\mathbb{R}^{16\times32\times32}$, kernel: $\mathbb{R}^{16\times16\times3\times3} \rightarrow \mathbb{R}^{16\times32\times32}$) - BN - ReLU | 16×16384 | 0, 1 |
| CONV (input: $\mathbb{R}^{16\times32\times32}$, kernel: $\mathbb{R}^{16\times16\times3\times3} \rightarrow \mathbb{R}^{16\times32\times32}$) - BN - ReLU | 16×16384 | 0, 1 |
| MP (input: $\mathbb{R}^{16\times32\times32}$, window: $\mathbb{R}^{16\times2\times2} \rightarrow \mathbb{R}^{16\times16\times16}$) | - | -, 2 |
| CONV (input: $\mathbb{R}^{16\times16\times16}$, kernel: $\mathbb{R}^{16\times32\times3\times3} \rightarrow \mathbb{R}^{32\times16\times16}$) - BN - ReLU | 16×8192 | 0, 1 |
| CONV (input: $\mathbb{R}^{32\times16\times16}$, kernel: $\mathbb{R}^{32\times32\times3\times3} \rightarrow \mathbb{R}^{32\times16\times16}$) - BN - ReLU | 16×8192 | 0, 1 |
| CONV (input: $\mathbb{R}^{32\times16\times16}$, kernel: $\mathbb{R}^{32\times32\times3\times3} \rightarrow \mathbb{R}^{32\times16\times16}$) - BN - ReLU | 16×8192 | 0, 1 |
| MP (input: $\mathbb{R}^{32\times16\times16}$, window: $\mathbb{R}^{32\times2\times2} \rightarrow \mathbb{R}^{32\times8\times8}$) | - | NA, 2 |
| CONV (input: $\mathbb{R}^{32\times8\times8}$, kernel: $\mathbb{R}^{32\times48\times3\times3} \rightarrow \mathbb{R}^{48\times6\times6}$) - BN - ReLU | 32×1728 | NA, 1 |
| CONV (input: $\mathbb{R}^{48\times6\times6}$, kernel: $\mathbb{R}^{48\times48\times3\times3} \rightarrow \mathbb{R}^{48\times4\times4}$) - BN - ReLU | 48×1728 | NA, 1 |
| CONV (input: $\mathbb{R}^{48\times4\times4}$, kernel: $\mathbb{R}^{48\times64\times3\times3} \rightarrow \mathbb{R}^{64\times2\times2}$) - BN - ReLU | 48×2304 | NA, 1 |
| MP (input: $\mathbb{R}^{64\times2\times2}$, window: $\mathbb{R}^{64\times2\times2} \rightarrow \mathbb{R}^{64\times1\times1}$) | NA | NA, 2 |
| FC ($64 \rightarrow 10$) - BN | 10 | NA, NA |

the user directly interacts with the model owner, through cryptographic protocols to obtain the inference result. These protocols ensure that the private model parameters cannot be learned by the client and the private user input cannot be exposed to the server. These works require the user and the model owner to be actively online for synchronous interactions, and to have symmetric computing capabilities, which are hard to be satisfied in practice especially for mobile user clients. Furthermore, most of these works involve heavy cryptographic techniques such homomorphic encryption and/or garbled circuits in the online execution of the cryptographic protocols. When deployed for mobile users, they will result in significant performance overheads.

Some other works [19], [20], [52] leverage the two-server model to carry out the computation of secure inference through tailored protocols, freeing the model owner and the client from active online participation. These secure inference protocols outsourced to the two servers, compared to the above mentioned interactive protocol, require to protect the neural network model and the client input simultaneously. However, these works still involve heavy cryptography during the secure inference procedure among the two servers. Specifically, they rely on expensive garbled circuit based approaches to support secure comparison as required in non-polynomial functions of neural networks such as the ReLU function and max pooling. Moreover, the works [20], [52] are designed for special binarized/ternarized NNs (BNN/TNN) with $\{0,1\}/\{-1,0,1\}$ weights, where their secure protocols cannot support generic CNNs with real-valued weights and more complicated layer functions. `Sonic` adopts a similar two-server model, yet fully relies on the lightweight secret sharing technique to build a customized protocol for efficient secure neural network inference services in the cloud.

There has been some works [17], [35], [53], [54], [55] focusing on efficient secure inference with three or four servers, which has much higher real-world deployment complexity compared to the two-server model. Among all prior works, we are aware that some systems [35], [41], [55] also only uses secret sharing, yet their protocols are specially designed under a more complex *three-server* setting [35], [55] where three servers interact with each other in the online inference procedure, or for a non-outsourcing setting that requires *continuous interactions* between the client and the service provider [41]. Table 17 gives a high-level comparison of `Sonic` with prior works.

### 7.2 Privacy-Preserving Machine Learning in Cloud computing

A rich body of work has explored privacy-preserving machine learning applications in cloud computing. Some of these works ensure the privacy resorting to cryptographic approaches (secure multiparty computation, homomorphic encryption) for various outsourced ML applications, like ridge regression and logistic regression [19], [56], decision trees [16], federated learning [57], video classification via CNNs [58]. A common rationale of these approaches is to design specialized cryptographic protocols to meet the certain needs of different applications. For example, POSEIDON [57] employs multiparty lattice-based fully homomorphic encryption for a quantum-resistant federated learning. Some other works utilize differential privacy techniques [27], [28], [29], [30] or rely on the trusted processors (e.g., SGX) [59], [60] for privacy preservation, such as the oblivious video analytics as a cloud service [59] and XGBoost learning [60]. Meanwhile, some other works [61] focus on an orthogonal aspect, i.e., verifying the integrity of machine leaning computation, but they do not guarantee the user data and model confidentiality.

### 7.3 Adversarial Machine Learning Attacks

There have been adversarial machine learning attacks [7], [8], [25], [26] that attempt to infer private information about the NN model and the training dataset via blackbox oracle access to the inference procedure. One major class of attacks are the membership inference attacks [8], [26], where an attacker aims to discover the presence of a particular record in the training dataset via querying the NN models in a black-box way[1]. Another class of attacks are the model inversion attacks [7], [62], which can be abused to infer the (hidden) sensitive attributes of the input data through the API access to the model. Apart from the inference attacks, there exist other attacks that try to steal specific information about the NN models, such as the model stealing attack [25], and hyperparameter stealing attack [63].

Defenses against those attacks are active research areas complementary to secure NN inference that we target in this paper. One mitigation approach is to limit the private information memorized by the NN model. A common strategy is to leverage differentially private learning [27], [28], [29], [30], so as to bound the privacy impact regarding whether or not a single data record is used to train the model. By injecting a

1. Membership inference attacks via white-box access [62] are out of the consideration as they requires auxiliary information (e.g., training losses) about training process.

TABLE 17
A high-level summary of different secure inference systems.

| | | | Heavy comp. cost | Heavy comm. cost[1] | Applicable for general CNNs[2] |
|---|---|---|---|---|---|
| Interactive 2PC Protocol (symmetric) | HE | CryptoNets [38], CryptoDL [51] | ● | ● | ○ |
| | | XONN [24] | ◐ | ○ | ○ |
| | Mixed | MiniONN [11] | ● | ● | ● |
| | | Gazelle [12] | ● | ◐ | ◐ |
| | | Delphi [13] | ◐ | ◐ | ● |
| | SS | MediSC [41] | ○ | ○ | ● |
| Outsourced 2PC Protocol | Mixed | SecureML [19] | ◐ | - | ● |
| | | Quotient [20] | ◐ | - | ○ |
| | | Leia [52] | ○ | ○ | ○ |
| | SS | `Sonic` (**our system**) | ○ | ○ | ● |
| Using Multiple Servers[3] | Mixed | ABY[3] [53], Trident [54] | ◐ | ○ | ● |
| | | Chameleon [17] | ◐ | ◐ | ● |
| | SS | SecureNN [35], CryptFlow [55] | ○ | ○ | ● |

[1] The communication cost is evaluated based on the results reported in prior works, and [19], [20] have not reported their inference bandwidth costs.
[2] Not fully support common CNN model architectures, which could downgrade inference accuracy.
[3] Require three or more servers to assist the online inference procedure.

calibrated amount of random noise to the NN model during training, the presence of a record in the training dataset and the effect of sensitive attribute on the prediction can be obfuscated [30]. Apart from using differential privacy techniques, some other ML methods have been proposed to reduce the private information given to the adversary via modifying the network and/or prediction, such as regularization [31], prediction API minimization [25], and perturbing the activation function [32]. Another approach is query auditing, where the feature space explored by queries [33], or the distribution of a batch of queries [34] is leveraged to detect adversarial ones. Indeed ensuring the confidentiality of the model weights could increase the overhead to successfully launch those attacks [34]. Such an approach compels an attacker to send more queries, and as a result, the adversarial queries are more likely to be detected.

## 8 Conclusion

In this paper, we present `Sonic`, an in-the-cloud lightweight secure neural network inference service. `Sonic` relaxes the end-user and model owner from being engaged in online secure inference procedure. `Sonic` is comprised of a series of secure layer functions purely relying on lightweight secret sharing techniques, each of which is highly customized for an efficient secure inference service in the cloud. `Sonic` provide strong guarantees on both user input and CNN model privacy. Experiments on common benchmark datasets demonstrates `Sonic`'s practical performance.

## References

[1] W. Liu, Z. Wang, X. Liu, N. Zeng, Y. Liu, and F. E. Alsaadi, "A survey of deep neural network architectures and their applications," *Neurocomputing*, vol. 234, pp. 11–26, 2017.
[2] S. Hu, Q. Wang, J. Wang, Z. Qin, and K. Ren, "Securing SIFT: privacy-preserving outsourcing computation of feature extractions over encrypted image data," *IEEE Transactions on Image Processing*, vol. 25, no. 7, pp. 3411–3425, 2016.
[3] Y. Zhang, C. Xu, H. Li, K. Yang, J. Zhou, and X. Lin, "Healthdep: An efficient and secure deduplication scheme for cloud-assisted ehealth systems," *IEEE Transactions on Industrial Informatics*, vol. 14, no. 9, pp. 4101–4112, 2018.
[4] H. Li, Y. Yang, Y. Dai, S. Yu, and Y. Xiang, "Achieving secure and efficient dynamic searchable symmetric encryption over medical cloud data," *IEEE Transactions on Cloud Computing*, vol. 8, no. 2, pp. 484–494, 2020.
[5] "Google Vision," Online at https://cloud.google.com/vision.
[6] X. Yi, R. Paulet, E. Bertino, and V. Varadharajan, "Practical approximate k nearest neighbor queries with location and query privacy," *IEEE Transactions on Knowledge and Data Engineering*, vol. 28, no. 6, pp. 1546–1559, 2016.
[7] M. Fredrikson, S. Jha, and T. Ristenpart, "Model inversion attacks that exploit confidence information and basic countermeasures," in *Proc. of ACM CCS*, 2015.
[8] R. Shokri, M. Stronati, C. Song, and V. Shmatikov, "Membership inference attacks against machine learning models," in *Proc. of IEEE S&P*, 2017.
[9] R. Cammarota, M. Schunter, A. Rajan, F. Boemer, Á. Kiss, A. Treiber, C. Weinert, T. Schneider, E. Stapf, A.-R. Sadeghi *et al.*, "Trustworthy ai inference systems: An industry research view," *arXiv preprint arXiv:2008.04449*, 2020.
[10] X. Yi, E. Bertino, F.-Y. Rao, K.-Y. Lam, S. Nepal, and A. Bouguettaya, "Privacy-preserving user profile matching in social networks," *IEEE Transactions on Knowledge and Data Engineering*, vol. 32, no. 8, pp. 1572–1585, 2019.
[11] J. Liu, M. Juuti, Y. Lu, and N. Asokan, "Oblivious neural network predictions via minionn transformations," in *Proc. of ACM CCS*, 2017.
[12] C. Juvekar, V. Vaikuntanathan, and A. Chandrakasan, "Gazelle: A low latency framework for secure neural network inference," in *Proc. of 27th USENIX Security*, 2018.
[13] P. Mishra, R. Lehmkuhl, A. Srinivasan, W. Zheng, and R. A. Popa, "Delphi: A cryptographic inference service for neural networks," in *Proc. of 29th USENIX Security*, 2020.
[14] M. Atallah, M. Bykova, J. Li, K. Frikken, and M. Topkara, "Private collaborative forecasting and benchmarking," in *Proc. of WPES*, 2004.
[15] D. Beaver, "Efficient multiparty protocols using circuit randomization," in *Proc. of Crypto*, 1991.
[16] Y. Zheng, H. Duan, and C. Wang, "Towards secure and efficient

outsourcing of machine learning classification," in *Proc. of ESORICS*, 2019.

[17] M. S. Riazi, C. Weinert, O. Tkachenko, E. M. Songhori, T. Schneider, and F. Koushanfar, "Chameleon: A hybrid secure computation framework for machine learning applications," in *Proc. of AsiaCCS*, 2018.

[18] "Amazon Rekognition," Online at https://aws.amazon.com/rekognition.

[19] P. Mohassel and Y. Zhang, "Secureml: A system for scalable privacy-preserving machine learning," in *Proc. of IEEE S&P*, 2017.

[20] N. Agrawal, A. Shahin Shamsabadi, M. J. Kusner, and A. Gascón, "Quotient: two-party secure neural network training and prediction," in *Proc. of ACM CCS*, 2019.

[21] Y. Zheng, H. Duan, and C. Wang, "Learning the truth privately and confidently: Encrypted confidence-aware truth discovery in mobile crowdsensing," *IEEE Trans. on Information Forensics and Security*, vol. 13, no. 10, pp. 2475–2489, 2018.

[22] B. Knott, S. Venkataraman, A. Hannun, S. Sengupta, M. Ibrahim, and L. van der Maaten, "Crypten: Secure multi-party computation meets machine learning," in *Proceedings of the NeurIPS Workshop on Privacy-Preserving Machine Learning*, 2020.

[23] Cape Privacy, "Tf encrypted: Encrypted deep learning in tensorflow." online at https://tf-encrypted.io/, 2020.

[24] M. S. Riazi, M. Samragh, H. Chen, K. Laine, K. Lauter, and F. Koushanfar, "Xonn: Xnor-based oblivious deep neural network inference," in *Proc. of 28th USENIX Security*, 2019.

[25] F. Tramèr, F. Zhang, A. Juels, M. K. Reiter, and T. Ristenpart, "Stealing machine learning models via prediction apis," in *25th {USENIX} Security Symposium ({USENIX} Security 16)*, 2016, pp. 601–618.

[26] C. Song, T. Ristenpart, and V. Shmatikov, "Machine learning models that remember too much," in *Proceedings of the 2017 ACM SIGSAC Conference on computer and communications security*, 2017, pp. 587–601.

[27] R. Shokri and V. Shmatikov, "Privacy-preserving deep learning," in *Proceedings of the 22nd ACM SIGSAC conference on computer and communications security*, 2015, pp. 1310–1321.

[28] L. Yu, L. Liu, C. Pu, M. E. Gursoy, and S. Truex, "Differentially private model publishing for deep learning," in *Proc. of S&P*. IEEE, 2019.

[29] R. Iyengar, J. P. Near, D. Song, O. Thakkar, A. Thakurta, and L. Wang, "Towards practical differentially private convex optimization," in *2019 IEEE Symposium on Security and Privacy (SP)*. IEEE, 2019, pp. 299–316.

[30] B. Jayaraman and D. Evans, "Evaluating differentially private machine learning in practice," in *28th {USENIX} Security Symposium ({USENIX} Security 19)*, 2019, pp. 1895–1912.

[31] N. Carlini, C. Liu, Ú. Erlingsson, J. Kos, and D. Song, "The secret sharer: Evaluating and testing unintended memorization in neural networks," in *28th {USENIX} Security Symposium ({USENIX} Security 19)*, 2019, pp. 267–284.

[32] T. Lee, B. Edwards, I. Molloy, and D. Su, "Defending against neural network model stealing attacks using deceptive perturbations," in *2019 IEEE Security and Privacy Workshops (SPW)*. IEEE, 2019, pp. 43–49.

[33] M. Kesarwani, B. Mukhoty, V. Arya, and S. Mehta, "Model extraction warning in mlaas paradigm," in *Proceedings of the 34th Annual Computer Security Applications Conference*, 2018, pp. 371–380.

[34] M. Juuti, S. Szyller, S. Marchal, and N. Asokan, "Prada: protecting against dnn model stealing attacks," in *2019 IEEE European Symposium on Security and Privacy (EuroS&P)*. IEEE, 2019, pp. 512–527.

[35] S. Wagh, D. Gupta, and N. Chandran, "Securenn: 3-party secure computation for neural network training," *Proc. of PETS*, 2019.

[36] S. Ioffe and C. Szegedy, "Batch normalization: Accelerating deep network training by reducing internal covariate shift," *arXiv preprint arXiv:1502.03167*, 2015.

[37] "Pytorch for densenet," Online at https://github.com/pytorch/vision/blob/master/torchvision/models/densenet.py.

[38] R. Gilad-Bachrach, N. Dowlin, K. Laine, K. Lauter, M. Naehrig, and J. Wernsing, "Cryptonets: Applying neural networks to encrypted data with high throughput and accuracy," in *Proc. of ICML*, 2016.

[39] Q. Lou and L. Jiang, "She: A fast and accurate deep neural network for encrypted data," in *Advances in Neural Information Processing Systems*, 2019, pp. 10 035–10 043.

[40] D. Harris, "A taxonomy of parallel prefix networks," in *The Thrity-Seventh Asilomar Conference on Signals, Systems & Computers, 2003*, vol. 2. IEEE, 2003, pp. 2213–2217.

[41] X. Liu, Y. Zheng, X. Yuan, and X. Yi, "Medisc: Towards secure and lightweight deep learning as a medical diagnostic service," in *European Symposium on Research in Computer Security*. Springer, 2021, pp. 519–541.

[42] A. Patra, T. Schneider, A. Suresh, and H. Yalame, "Aby2. 0: Improved mixed-protocol secure two-party computation," in *30th {USENIX} Security Symposium ({USENIX} Security 21)*, 2021.

[43] Y. Zheng, C. Wang, R. Wang, H. Duan, and S. Nepal, "Optimizing secure decision tree inference outsourcing," *arXiv preprint arXiv:2111.00397*, 2021.

[44] "Execution order of ReLU and Max-Pooling." Online at https://github.com/tensorflow/tensorflow/issues/3180.

[45] F. Boemer, R. Cammarota, D. Demmler, T. Schneider, and H. Yalame, "Mp2ml: a mixed-protocol machine learning framework for private inference," in *Proceedings of the 15th International Conference on Availability, Reliability and Security*, 2020, pp. 1–10.

[46] D. Demmler, T. Schneider, and M. Zohner, "Aby-a framework for efficient mixed-protocol secure two-party computation." in *Proc. of NDSS*, 2015.

[47] O. Goldreich, S. Micali, and A. Wigderson, "How to play any mental game or a completeness theorem for protocols with honest majority," in *Proc. of STOC*, 1987.

[48] A. Romero, N. Ballas, S. E. Kahou, A. Chassang, C. Gatta, and Y. Bengio, "Fitnets: Hints for thin deep nets," *arXiv preprint arXiv:1412.6550*, 2014.

[49] N. Chandran, D. Gupta, A. Rastogi, R. Sharma, and S. Tripathi, "Ezpc: programmable, efficient, and scalable secure two-party computation for machine learning," *ePrint Report*, vol. 1109, 2017.

[50] P. Ren, Y. Xiao, X. Chang, P.-Y. Huang, Z. Li, X. Chen, and X. Wang, "A comprehensive survey of neural architecture search: Challenges and solutions," *arXiv preprint arXiv:2006.02903*, 2020.

[51] E. Hesamifard, H. Takabi, and M. Ghasemi, "Cryptodl: Deep neural networks over encrypted data," *arXiv preprint arXiv:1711.05189*, 2017.

[52] X. Liu, B. Wu, X. Yuan, and X. Yi, "Leia: A lightweight cryptographic neural network inference system at the edge." *IACR Cryptol. ePrint Arch.*, vol. 2020, p. 463, 2020.

[53] P. Mohassel and P. Rindal, "Aby3: A mixed protocol framework for machine learning," in *Proc. of ACM CCS*, 2018.

[54] H. Chaudhari, R. Rachuri, and A. Suresh, "Trident: Efficient 4pc framework for privacy preserving machine learning," in *Proc. of NDSS*, 2020.

[55] N. Kumar, M. Rathee, N. Chandran, D. Gupta, A. Rastogi, and R. Sharma, "Cryptflow: Secure tensorflow inference," in *Proc. of IEEE SP*, 2020.

[56] V. Nikolaenko, U. Weinsberg, S. Ioannidis, M. Joye, D. Boneh, and N. Taft, "Privacy-preserving ridge regression on hundreds of millions of records," in *Proc. of IEEE S&P*, 2013.

[57] S. Sav, A. Pyrgelis, J. R. Troncoso-Pastoriza, D. Froelicher, J.-P. Bossuat, J. S. Sousa, and J.-P. Hubaux, "Poseidon: Privacy-preserving federated neural network learning," *Proc. of NDSS*, 2022.

[58] S. Pentyala, R. Dowsley, and M. De Cock, "Privacy-preserving video classification with convolutional neural networks," *arXiv preprint arXiv:2102.03513*, 2021.

[59] R. Poddar, G. Ananthanarayanan, S. Setty, S. Volos, and R. A. Popa, "Visor: Privacy-preserving video analytics as a cloud service," in *29th {USENIX} Security Symposium ({USENIX} Security 20)*, 2020, pp. 1039–1056.

[60] A. Law, C. Leung, R. Poddar, R. A. Popa, C. Shi, O. Sima, C. Yu, X. Zhang, and W. Zheng, "Secure collaborative training and inference for xgboost," in *Proc. of the 2020 Workshop on Privacy-Preserving Machine Learning in Practice*, 2020.

[61] L. Zhao, Q. Wang, C. Wang, Q. Li, C. Shen, and B. Feng, "Veriml: Enabling integrity assurances and fair payments for machine learning as a service," *IEEE Transactions on Parallel and Distributed Systems*, pp. 1–1, 2021.

[62] S. Yeom, I. Giacomelli, M. Fredrikson, and S. Jha, "Privacy risk in machine learning: Analyzing the connection to overfitting," in *2018 IEEE 31st Computer Security Foundations Symposium (CSF)*. IEEE, 2018, pp. 268–282.

[63] B. Wang and N. Z. Gong, "Stealing hyperparameters in machine learning," in *2018 IEEE Symposium on Security and Privacy (SP)*. IEEE, 2018, pp. 36–52.

**Xiaoning Liu** is currently a Ph.D. candidate at the School of Computer Science and Software Engineering, RMIT University. She received her B.E. degree in computer science and technology from Henan University in 2012, and the M.S. degree in computer science from City University of Hong Kong in 2013. Her research interests include privacy-preserving data mining and machine learning.

**Yifeng Zheng** is an assistant professor with the School of Computer Science and Technology, Harbin Institute of Technology, Shenzhen, China. He received the PhD degree in computer science from City University of Hong Kong, Hong Kong, in 2019. He worked as a postdoc in the Commonwealth Scientific and Industrial Research Organization (CSIRO), Australia, and City University of Hong Kong, respectively. His work has appeared in prestigious venues such as ESORICS, ACM AsiaCCS, DSN, IEEE INFOCOM, IEEE ICDCS, IEEE Transactions on Dependable and Secure Computing, IEEE Transactions on Information Forensics and Security, and IEEE Transactions on Multimedia, and IEEE Transactions on Services Computing. His current research interests are focused on security and privacy related to cloud computing, IoT, machine learning, and multimedia.

**Xingliang Yuan** is currently a Senior Lecturer (aka US Associate Professor) at the Department of Software Systems and Cybersecurity in the Faculty of Information Technology, Monash University, Australia. His research interests include data security and privacy, secure networked system, machine learning security and privacy, confidential computing. His research has been supported by Australian Research Council, CSIRO Data61, and Oceania Cyber Security Centre. In the past few years, his work has appeared in prestigious venues in cybersecurity, computer networks, and distributed systems, such as ACM CCS, NDSS, IEEE INFOCOM, IEEE TDSC, IEEE TIFS, and IEEE TPDS. He was the recipient of the Dean's Award for Excellence in Research by an Early Career Researcher at Monash Faculty of IT in 2020. He received the best paper award in the European Symposium on Research in Computer Security (ESORICS) 2021, the IEEE Conference on Dependable and Secure Computing (IDSC) 2019, and the IEEE International Conference on Mobility, Sensing and Networking (MSN) 2015.

**Xun Yi** is currently a professor with the School of Science, RMIT University, Australia. His research interests include applied cryptography, computer and network security, mobile and wireless communication security, and privacy-preserving data mining. He has published more than 150 research papers in international journals, such as the IEEE Transactions on Computers, IEEE Transactions on Parallel and Distributed Systems, IEEE Transactions on Knowledge and Data Engineering, IEEE Transactions on Wireless Communications, IEEE Transactions on Dependable and Secure Computing, IEEE Transactions on Information Forensics and Security, IEEE Transactions on Circuits and Systems, IEEE Transactions on Vehicular Technology, IEEE Communication Letters, IEE Electronic Letters, and conference proceedings. He has ever undertaken program committee members for more than 30 international conferences. Recently, he has led a few of Australia Research Council (ARC) Discovery Projects. Since 2014, he has been an associate editor of the IEEE Transactions on Dependable and Secure Computing.